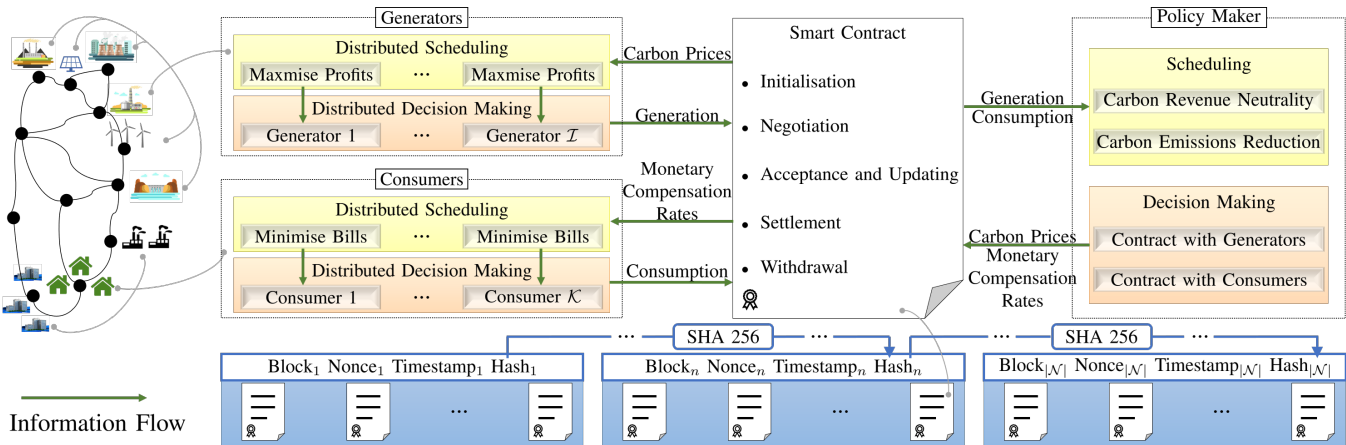


# Graphical Abstract

## Consumer-centric decarbonization framework using Stackelberg game and Blockchain

WeiQi Hua, Jing Jiang, Hongjian Sun, Fei Teng, Goran Strbac



# Consumer-centric decarbonization framework using Stackelberg game and Blockchain

WeiQi Hua<sup>a</sup>, Jing Jiang<sup>b</sup>, Hongjian Sun<sup>c,\*</sup>, Fei Teng<sup>d</sup>, Goran Strbac<sup>d</sup>

<sup>a</sup>*School of Engineering, Cardiff University, Cardiff, CF24 3AA, UK*

<sup>b</sup>*Department of Mathematics, Physics and Electrical Engineering, University of Northumbria, Newcastle, NE1 8ST, UK*

<sup>c</sup>*Department of Engineering, Durham University, DH1 3LE, Durham, UK*

<sup>d</sup>*Department of Electrical and Electronic Engineering, Imperial College London, London, UK*

---

## Abstract

Energy policy is too often not designed for energy consumers in a low-cost and consumer-friendly manner. This paper proposes a novel Stackelberg game and Blockchain-based framework that enables consumer-centric decarbonization by automating iterative negotiations between policy makers and consumers or generators to reduce carbon emissions. This iterative negotiation is modeled as a Stackelberg game-theoretic problem, and securely facilitated by Blockchain technologies. The policy maker formulates carbon prices and monetary compensation rates to dynamically incentivize the carbon reduction, whereas consumers and generators schedule their power profiles to minimize bills and maximize profits of generation, respectively. The negotiating agreement is yielded by reaching a Stackelberg equilibrium. The exchanged information and controlling functions are realized by using smart contracts of Blockchain technologies. Case studies of GB power systems show that the proposed framework can incentivize 9% more bill savings for consumers and 45.13% more energy generation from renewable energy sources. As a consumer-centric decarbonization framework, it can at least reduce carbon emissions by 40%.

**Keywords:** Blockchain, carbon reduction, power system scheduling, renewable energy, smart contracts, game theory.

---

## 1. Introduction

To reduce carbon emissions, policy makers look for means of encouraging low-carbon energy generation, such as renewable energy sources, and shaping consumer behaviors [1]. The long-term market based policy design for decarbonizing the energy sector has been well studied, e.g., the carbon pricing scheme [2], contract for difference [3], and feed-in-tariff [4], through which the monetary incentive can directly stimulate the integration of renewable energy sources. The carbon pricing quantifies how much climate levy is incurred when a pollutant emitter, e.g., electricity generator, produces per unit of carbon emissions due to the combustion of fossil fuels. Since purchasing the climate levy accounts for a portion of generating costs, carbon pricing can enforce generators to compensate the environmental damage in a monetary manner. Two standard mechanisms of the carbon pricing scheme are the carbon tax and emissions trading scheme. The carbon tax levies a fixed tax rate on per unit of carbon emissions and this rate is determined by the marginal damage cost of carbon emissions to the society [5]. By contrast, the emissions trading scheme allocates a fixed amount of carbon allowance [6]. The pollutant emitters are obliged to have the enough carbon allowance covering their carbon emissions. The surplus or deficiency of carbon allowance can be traded among pollutant emitters. By May 2021,

the carbon pricing scheme has been implemented in 37 countries and 27 sub-national jurisdictions, of which 28 countries or sub-national jurisdictions employ the carbon tax, 29 countries or sub-national jurisdictions employ the emissions trading scheme, and others employ the combination of both [7].

Nonetheless, the long-term carbon pricing scheme cannot react to the dynamic changes of carbon emissions incurred by intermittent generation, and barely consider the role of consumers whose energy consumption is a primary driver for the carbon emissions from generators. As a consequence, an inappropriate carbon pricing scheme would inefficiently deliver the low carbon target. As indicated by the report of the UK parliament [8], if carbon prices lie below the social cost of carbon, it would fail to achieve the target of carbon reduction; If carbon prices in one region are higher than the carbon prices in another region, the market competitiveness of generators in the high-price region would be harmed. To overcome the issue of an inappropriate carbon pricing scheme, further research focused on developing dynamic carbon pricing schemes by considering the participation of consumers. Wang *et al.* [9] proposed a bilateral carbon trading mechanism with active demand side management for facilitating the low carbon energy dispatch. In [10], a dynamic emissions trading system was designed under five energy dispatch modes to promote renewable energy generation for decarbonizing power systems. Researchers in [11] investigated the impacts of the carbon pricing scheme on heterogeneous groups of households from the US consumers and provided a solution to redistributing the revenue from the carbon pricing scheme. Fan *et al.* [12] developed a consumer-centric emissions trading

---

\*Corresponding author.

Email addresses: huaw5@cardiff.ac.uk (WeiQi Hua),  
jing.jiang@northumbria.ac.uk (Jing Jiang),  
hongjian.sun@durham.ac.uk (Hongjian Sun), f.teng@imperial.ac.uk  
(Fei Teng), g.strbac@imperial.ac.uk (Goran Strbac)

scheme as the personal carbon trading, and investigated the response of consumers to both short-term and long-term changes of carbon prices. Xu and Hobbs [13] incorporated the factors of the dynamic generation mix, net load distribution, and transmission limits into the carbon pricing scheme, in order to reduce carbon emissions without raising costs of consumers and eliminate regional difference of carbon prices.

The Stackelberg game theory has drawn increasing attention in modeling the decision-making of stakeholders in power systems, in particular for encouraging consumers' involvement. Yu *et al.* [14] modeled a hierarchical decision-making of a power grid operator, service providers, and consumers as a Stackelberg game to incentivize the demand response of consumers in power systems. Li *et al.* [15] proposed a Stackelberg game based optimization framework to schedule aggregated demand response under uncertainties caused by renewable energy generation, in which an integrated energy operator at the leader level maximizes its profits while consumers at the follower level minimize their bills. In [16], a bi-level economic-environmental equilibrium model was designed to optimize the dispatch of integrated energy systems for reducing carbon emissions. However, as indicated by the research in [17], all of these approaches require significant information exchange among relevant stakeholders and pose new challenges in terms of information trustiness and cyber-security.

The emergence of smart contracts of Blockchain technologies [18] has the potential to establish a standardized negotiation protocol in a secure and trusted way. The smart contracts automatically perform programmable functions for setting out negotiation and self-enforcing execution with duplicable, secure, and verifiable features [19]. Applying Blockchains and smart contracts into power systems has been well documented too, but in terms of system operations [20, 21], planning [17, 22], and energy trading [23]. In [20], a decentralized consensus algorithm was developed that used Blockchain technologies to improve the efficiency, transparency, security, and trust of performing optimal power flow analyses. Liang *et al.* [21] proposed a distributed Blockchain framework to improve the self-defensive capability of power systems, in which the meter measurements were enclosed into blocks to prevent cyber-attacks. Thomas *et al.* [17] designed a general form of smart contracts for controlling the energy transfer between different distribution networks. Li *et al.* [22] used smart contracts to design a distributed hybrid energy system with residential, commercial, and industrial consumers for supporting demand side management programmes. Luo *et al.* [23] incorporated a multi-agent system into a Blockchain-based transaction settlement mechanism to ensure the security and trustiness of distributed energy trading.

Different from the literature, the key research questions to be addressed by this paper are:

1. How to design carbon prices that dynamically affect the mix of energy generation whilst ensuring monetary compensations effectively encourage consumers' behaviors to achieve the decarbonization goal?
2. How to enhance the automation, standardization, self-

enforcement, and security of the negotiations among relevant stakeholders by using Blockchain based smart contracts?

3. What are the benefits when policy makers, consumers and generators iteratively negotiate their strategies in terms of reducing carbon emissions, saving bills, and generating more profits, respectively?

To address the first question, a novel consumer-centric and negotiation-based framework is proposed in which the carbon prices and monetary compensation rates can dynamically update with the power profiles of both consumers and generators for reducing carbon emissions. The iterative negotiations between the policy maker and generators/consumers reach an agreement through finding an equilibrium of the Stackelberg game-theoretic problem. To address the second question, a Blockchain based platform is developed to integrate the exchanged information and controlling functions of the power system scheduling into the data structures, nodes, and smart contracts of Blockchain networks. The consequences of potential cyber-attacks to both smart contracts and meter readings, and how the developed Blockchain based platform can prevent these attacks are discussed. Case studies demonstrate that the proposed framework of iterative negotiation outperforms other approaches without the negotiation [24] or without the scheduling in terms of the benefits of all power system participants, which addresses the third question.

The rest of this paper is organized as follows. Section 2 introduces the problem formulations to analyze the strategies of the policy maker, generators, and consumers by using a Stackelberg game-theoretic model. Section 3 discusses the data structure, node types, and smart contracts of the designed Blockchain based negotiation platform, and demonstrates how it protects power system participants from attacks. The results of case studies are provided in Section 4. Section 5 concludes this paper and lists the future works.

## 2. Problem formulations

The interactions and decision making of the policy maker, generators, and consumers are presented in Fig. 1. The policy maker incentivizes the carbon reduction through charging the carbon allowance from generators and providing the monetary compensation for consumers, including residential, commercial, and industrial users. For those generators which are willing to reduce their carbon costs and consumers which are willing to earn the monetary compensation, they would reshape their power profiles as their responses. Receiving these responses, the policy maker further adjusts the policy decisions in achieving the targeted carbon reduction. These interactions iteratively proceed until reaching an equilibrium agreement at which neither the policy maker nor any generator/consumer wants to deviate. The process of the iterative negotiation and reaching an equilibrium agreement is modeled by a two-level Stackelberg game-theoretic problem with one leader (the policy maker) and multiple followers (generators and consumers). The proposed

model is implemented in the day-ahead market to enable the energy scheduling and negotiation for the following day.

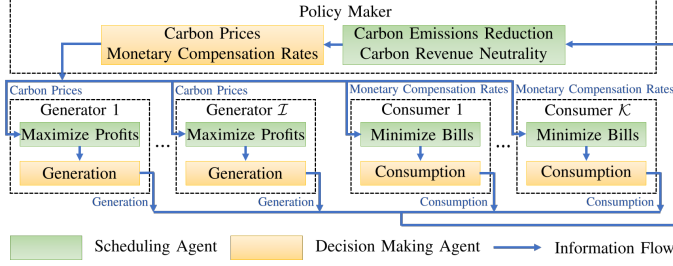


**Fig. 1.** Proposed framework of interactions and decision making of the policy maker, generators, and consumers. Each participant possesses two types of agents for scheduling and decision making as indicated by the green and yellow colors.

The functions of the decision making and information exchange are performed by an agent based system. Each participant (i.e., the policy maker, a generator, or a consumer) possesses two agents: a scheduling agent and a decision making agent, as indicated by green and yellow colors in Fig. 1. The functions of the scheduling agents include: 1) optimizing a participant's objective functions when receiving the decisions from the other level; 2) sending the optimal decisions to the decision making agents. The functions of the decision making agents include: 1) confirming whether a participant accepts the optimal decisions; 2) initializing and updating the confirmed carbon prices and monetary compensation rates for the policy maker; 3) submitting the confirmed power profiles of generators/consumers for negotiating with the policy maker.

*Remark 1:* The retail electricity prices and wholesale electricity prices are determined by the market operator. The power balance and system constraints are managed by the system operator. These roles are beyond the scope of this framework.

*Remark 2:* The modeled interactions and decision making of the stakeholders (policy maker, generators, and consumers) lead to a general framework which can be implemented to a specific energy sector. For instance in the GB energy sector, the policy maker represents the Department for Business, Energy and Industrial Strategy (BEIS) which sets the carbon pricing scheme and issues the low carbon incentives [25]. The generators represent 1307 power stations owned by 55 generation companies as outlined in the Digest of UK Energy Statistics (DUKES) 2021 report [26]. The consumers represent 29 spatially explicit energy consumption from residential, commercial, and industrial users in GB as identified by [27]. Two standardized types of agents (scheduling agent and decision making agent) aim to represent the acting process, i.e., making decisions in achieving certain targets, of these stakeholders.

Let  $\mathcal{I}$ ,  $\mathcal{K}$ ,  $\mathcal{L}$ ,  $\mathcal{T}$  denote the sets of generators, loads, transmission lines and scheduling time, indexed by integers  $i$ ,  $k$ ,  $l$ , and  $t$ , respectively, and  $|\mathcal{I}|$ ,  $|\mathcal{K}|$ ,  $|\mathcal{L}|$ , and  $|\mathcal{T}|$  denote the corresponding total numbers. The ranges of these integers are  $i \in [1, |\mathcal{I}|]$ ,  $k \in [1, |\mathcal{K}|]$ ,  $l \in [1, |\mathcal{L}|]$ , and  $t \in [1, |\mathcal{T}|]$ , respectively. Let the real number  $\Delta t$  denote the scheduling interval. For the 0.5 h of the fixed scheduling interval in our research, we have  $(\Delta t, |\mathcal{T}|) = (0.5, 48)$ .

## 2.1. The role of generators

Generators aim to maximize their profits by strategically deciding power outputs and incurred carbon emissions in responding to the carbon prices. The profit of a generator is the difference between the revenue of selling the electricity to the wholesale markets and the generating costs as

$$\max_{p_{i,t}, r_{i,t}} f_i(p_{i,t}, r_{i,t}) := \sum_{t \in \mathcal{T}} \{p_{i,t} \cdot \Delta t \cdot \pi_{ws,t} - [c_{\text{carbon},i}(r_{i,t}) + c_i(p_{i,t})]\}, \quad (1)$$

s.t.

$$p_i^{\min} \leq p_{i,t} \leq p_i^{\max}, \forall t \in [1, |\mathcal{T}|], i \in [1, |\mathcal{I}|], \quad (2)$$

$$-\Delta p_i^{\text{down}} \leq p_{i,t} - p_{i,t-1} \leq \Delta p_i^{\text{up}}, \forall t \in [2, |\mathcal{T}|], i \in [1, |\mathcal{I}|], \quad (3)$$

where  $f_i(\cdot)$  is the objective function of the profit for the generator  $i$ , the real numbers  $p_{i,t}$  and  $r_{i,t}$  are the decision variables representing the power generation and incurred carbon emission rate (with a unit of ton/h) of the generator  $i$  at the scheduling time  $t$ , respectively, and  $c_{\text{carbon},i}(\cdot)$  and  $c_i(\cdot)$  are the functions of the carbon cost and other operating costs for the generator  $i$ , respectively. Other real numbers  $\pi_{ws,t}$ ,  $p_i^{\min}$ ,  $p_i^{\max}$ ,  $\Delta p_i^{\text{down}}$ , and  $\Delta p_i^{\text{up}}$  are fixed inputs, in which  $\pi_{ws,t}$  is the wholesale electricity price at the scheduling time  $t$  purchased by the electricity suppliers,  $p_i^{\min}$  and  $p_i^{\max}$  are the minimum and maximum levels of the power generation from the generator  $i$ , respectively,  $\Delta p_i^{\text{down}}$  and  $\Delta p_i^{\text{up}}$  are the maximum down-ramp and up-ramp rates of the generator  $i$ , respectively. Equation (2) describes the power output constraint and equation (3) describes the ramp rate constraint.

As one of the generating costs, the carbon cost quantifies how much a generator pays for the allowance of pollutant emissions, and is subject to the variations of carbon prices. Incorporating the carbon pricing into the generating costs would incentivize conventional fossil fuel based generators to be replaced by the renewable generators. To analyze the incentive effects of the carbon pricing, the carbon cost is set aside from the operating costs. The function of the carbon cost can be modeled as

$$c_{\text{carbon},i}(r_{i,t}) := r_{i,t} \cdot \Delta t \cdot \pi_{\text{carbon},t}, \forall t \in [1, |\mathcal{T}|], i \in [1, |\mathcal{I}|], \quad (4)$$

where the real number  $\pi_{\text{carbon},t}$  is the fixed input representing the carbon price at the scheduling time  $t$  (with a unit of £/ton). The relationship between the carbon emission rate and power output of a generator is given by

$$r_{i,t} = p_{i,t} \cdot \rho_{i,t}, \forall t \in [1, |\mathcal{T}|], i \in [1, |\mathcal{I}|], \quad (5)$$

where the real number  $\rho_{i,t}$  is the fixed input representing the carbon emission intensity of the generator  $i$  at the scheduling time  $t$  (with a unit of ton/MWh). The value of  $\rho_{i,t}$  is determined by the source of a generator, which is evaluated as follows:

- The coal and gas are the dominant sources of carbon emissions. The marginal generators with these two sources would respond to the increasing power outputs from renewable energy sources by operating at the part-load state. This part-load operation would reduce the efficiency, which consumes more fossil

fuels and raises the carbon emission intensities. To consider this part-load impact, the dynamic carbon emission intensities for the coal and gas studied in [28] are used by our research as

$$\begin{aligned}\rho_{i,t} = & 6.4 \cdot \delta_{i,t}^6 - 29.0 \cdot \delta_{i,t}^5 + 54.7 \cdot \delta_{i,t}^4 - 56.1 \cdot \delta_{i,t}^3 + 33.9 \cdot \delta_{i,t}^2 \\ & - 12.0 \cdot \delta_{i,t} + 3.1, \forall t \in [1, |\mathcal{T}|], \text{ if the generator } i \text{ uses coal,} \\ & (6) \\ \rho_{i,t} = & 0.14 \cdot \delta_{i,t}^6 - 0.68 \cdot \delta_{i,t}^5 + 1.49 \cdot \delta_{i,t}^4 - 1.91 \cdot \delta_{i,t}^3 + 1.69 \cdot \delta_{i,t}^2 \\ & - 1.05 \cdot \delta_{i,t} + 0.71, \forall t \in [1, |\mathcal{T}|], \text{ if the generator } i \text{ uses gas,} \\ & (7)\end{aligned}$$

where the real number  $\delta_{i,t}$  is the fixed input representing the power factor of the generator  $i$  at the scheduling time  $t$ .

- The average carbon emission intensities [29] are used for the biomass and nuclear as

$$\rho_{i,t} = \rho_{\text{fuel},i} \cdot u_i / p_i, \forall t \in [1, |\mathcal{T}|], \text{ if the generator } i \text{ uses biomass or nuclear,} \quad (8)$$

where the real number  $\rho_{\text{fuel},i}$  is the fixed input representing the carbon emission intensity of the fuel used by the generator  $i$ , real number  $u_i$  is the fixed input representing the annual fuel usage of the generator  $i$ , and real number  $p_i$  is the fixed input representing annual power generation of the generator  $i$ .

- The carbon emissions of the wind, hydro and solar primarily arise in the manufacture and construction. Hence, the operational carbon emission intensities of these sources are assumed to be zero in our research as

$$\rho_{i,t} = 0, \forall t \in [1, |\mathcal{T}|], \text{ if the generator } i \text{ uses wind, hydro, and solar.} \quad (9)$$

Apart from the carbon cost, other operating costs include the costs of the operation, maintenance, and fuel [30] (the costs of the pre-development, construction, decommissioning, and waste are not considered in our operational scheduling problem). The coefficients of operating costs for each of energy sources are evaluated by the levelized costs of the electricity generation (LCoE) [31] which is the discounted lifetime costs of a specific energy source, and quantified by the ratio of the total costs of a source to the total expected amount of the electricity generation. The function of the other operating costs can be modeled as

$$c_i(p_{i,t}) := p_{i,t} \cdot \Delta t \cdot \mu_i, \forall t \in [1, |\mathcal{T}|], i \in [1, |\mathcal{I}|], \quad (10)$$

where the real number  $\mu_i$  is the fixed input representing the coefficient of the other operating costs of the generator  $i$ .

## 2.2. The role of consumers

Consumers aim to minimize their electricity bills by strategically deciding the consumption behaviors and incurred carbon emissions in responding to the low carbon incentive, which is modeled as

$$\min_{p_{k,t}, r_{k,t}} f_k(p_{k,t}, r_{k,t}) := \sum_{t \in \mathcal{T}} [p_{k,t} \cdot \Delta t \cdot \pi_t - \gamma_k(r_{k,t})], \quad (11)$$

s.t.

$$p_k^{\min} \leq p_{k,t} \leq p_k^{\max}, \forall t \in [1, |\mathcal{T}|], k \in [1, |\mathcal{K}|], \quad (12)$$

where  $f_k(\cdot)$  is the objective function of the electricity bill for the consumer  $k$ , the real numbers  $p_{k,t}$  and  $r_{k,t}$  are the decision variables representing the power consumption and incurred carbon emission rate of the consumer  $k$  at the scheduling time  $t$ , respectively, and  $\gamma_k(\cdot)$  is the function of the received monetary compensation by the consumer  $k$  for the carbon reduction. Other real numbers  $\pi_t$ ,  $p_k^{\min}$ , and  $p_k^{\max}$  are fixed inputs, in which  $\pi_t$  is the retail electricity price at the scheduling time  $t$  charged by the electricity suppliers, and  $p_k^{\min}$  and  $p_k^{\max}$  are the minimum and maximum power consumption levels of the consumer  $k$ , respectively. Equation (12) describes the constraint of the load levels.

To formulate the monetary compensation, how much carbon emissions are produced by generators when consuming per unit of energy at the specific time and load needs to be evaluated. This information can be tracked by the approach of the carbon emissions flow (CEF) as proposed in [32] by analyzing the topological structures and power flows of power networks. For the detailed approach, readers can refer to the Appendix A and [32]. Here, a key relationship between the consumption behaviors and incurred carbon emission rate is given as

$$r_{k,t} = p_{k,t} \cdot \frac{\sum_{l \in \mathcal{L}_k} p_{l,t}^{\text{in}} \cdot \rho_{l,t}^{\text{in}} + \sum_{i \in \mathcal{I}_k} p_{i,t} \cdot \rho_{i,t}}{\sum_{l \in \mathcal{L}_k} p_{l,t}^{\text{in}} + \sum_{i \in \mathcal{I}_k} p_{i,t}}, \forall t \in [1, |\mathcal{T}|], k \in [1, |\mathcal{K}|], \quad (13)$$

where the real numbers  $p_{l,t}^{\text{in}}$  and  $\rho_{l,t}^{\text{in}}$  are the fixed inputs representing the power inflow to a bus and incurred carbon emission intensity of the transmission line  $l$  at the scheduling time  $t$ , respectively (When  $p_{i,t}$  and  $p_{k,t}$  are determined,  $p_{l,t}^{\text{in}}$  can be obtained from the power flow analysis), and  $\mathcal{L}_k$  and  $\mathcal{I}_k$  are the sets of transmission lines and generators connected to the bus with the consumer  $k$ , respectively.

With the capability of tracking carbon emissions at the specific time and load, our research subsequently formulates a decentralized monetary compensation scheme. Incorporating the monetary compensation into the electricity bills would incentivize consumers to shift away or curtail their loads when the carbon emission rate is high. The following principles [33] need to be considered to formulate this monetary compensation scheme: 1) If the carbon emission rate after the policy maker's incentive is higher than or equal to that before the policy maker's incentive, a consumer will not receive any monetary compensation; 2) When the carbon emission rate before the policy maker's incentive, denoted as  $\bar{r}_{k,t}$ , is known, the monetary compensation should be monotonically decreasing to the carbon emission rate after the policy maker's incentive, i.e.,  $\partial \gamma_k(r_{k,t}, \bar{r}_{k,t}) / \partial r_{k,t} < 0$ ; 3) The consumers under the time and load with a higher carbon emission rate will receive more monetary compensation than the consumers under the time and load with a lower carbon emission rate, since the former is more urgent for the carbon mitigation. This means that the marginal monetary compensation should be monotonically increasing to the carbon emission rate before the policy maker's incentive,

i.e.,  $\partial^2 \gamma_k(r_{k,t}, \bar{r}_{k,t}) / \partial \bar{r}_{k,t}^2 > 0$ . Hence, the following function [33] which satisfies all these three principles is modeled as the decentralized monetary compensation.

$$\gamma_k(r_{k,t}, \bar{r}_{k,t}) := \begin{cases} \alpha_t \cdot \sqrt{(\bar{r}_{k,t} \cdot \Delta t)^2 - (r_{k,t} \cdot \Delta t)^2}, & \bar{r}_{k,t} > r_{k,t}, \\ 0, & \bar{r}_{k,t} \leq r_{k,t}, \end{cases} \quad (14)$$

$$\forall t \in [1, |\mathcal{T}|], k \in [1, |\mathcal{K}|],$$

where the real number  $\alpha_t$  is the fixed input (when the decision made by the policy maker) representing the monetary compensation rate at the scheduling time  $t$  (with a unit of £/ton).

### 2.3. The role of the policy maker

The policy maker aims to mitigate the total carbon emissions from power systems and facilitate the carbon revenue neutrality, by strategically deciding the targeted carbon reduction and adjusting the carbon prices and monetary compensation rates. According to the carbon footprint [32], the total carbon emission rate from power systems equals to the total carbon emission rate of generators, and is subject to the carbon emission conservation at any given time as

$$\sum_{i \in \mathcal{I}} r_{i,t} = \sum_{k \in \mathcal{K}} r_{k,t} + \sum_{l \in \mathcal{L}} r_{l,t} = \varrho \cdot \sum_{i \in \mathcal{I}} r_{i,t} + (1 - \varrho) \cdot \sum_{i \in \mathcal{I}} r_{i,t}, \quad \forall t \in [1, |\mathcal{T}|], \quad (15)$$

where the real number  $r_{l,t}$  is the fixed input (when power flow is determined) representing the carbon emission rate incurred by the power loss of the transmission line  $l$  at the scheduling time  $t$ , and real number  $\varrho$  is the fixed input representing the ratio of the carbon emission rate from the consumption side to the total carbon emission rate. Through solving the optimization problems of generators and consumers, the optimal carbon emission rates of every generator  $i$  and load  $k$  at the scheduling time  $t$ , denoted as  $r_{i,t}^*$  and  $r_{k,t}^*$ , respectively, can be obtained by the policy maker as fixed inputs. The policy maker then adjusts the carbon prices and monetary compensation rates to abate the total carbon emission rate of generators by  $\sum_{i \in \mathcal{I}} \Delta r_{i,t}$ ,  $\forall t \in [1, |\mathcal{T}|]$ . According to equation (15), the total carbon emission rate of consumers would be abated by

$$\sum_{k \in \mathcal{K}} \Delta r_{k,t} = \varrho \cdot \sum_{i \in \mathcal{I}} \Delta r_{i,t}, \quad \forall t \in [1, |\mathcal{T}|], \quad (16)$$

where the real numbers  $\Delta r_{i,t}$  and  $\Delta r_{k,t}$  are the decision variables representing the amounts of the reduced carbon emission rates of the generator  $i$  and load  $k$  at the scheduling time  $t$ , respectively.

Firstly, from the economic perspective, the carbon revenue neutrality defines that the revenue from the carbon pricing scheme should be redistributed as much as possible in a manner of the monetary incentive [34], which is one of the principles for guiding the policy maker to design a low carbon policy. In the context of our research, this means that the revenue of selling carbon allowances to generators needs to be redistributed to consumers by providing monetary compensations. Hence, the

objective function of the carbon revenue can be modeled as

$$f_n(\pi_{\text{carbon},t}, \alpha_t, \Delta r_{i,t}, \Delta r_{k,t}) := \sum_{t \in \mathcal{T}} \left\{ \sum_{i \in \mathcal{I}} c_{\text{carbon},i} (r_{i,t}^* - \Delta r_{i,t}) - \sum_{k \in \mathcal{K}} \gamma_k(r_{k,t}^* - \Delta r_{k,t}, r_{k,t}^*) \right\}, \quad (17)$$

where  $f_n(\cdot)$  is the objective function of the carbon revenue.

Secondly, from the environmental perspective, the policy marker should mitigate the total carbon emission rate from power systems. The objective function of the total carbon emission rate can be modeled as

$$f_c(\Delta r_{i,t}) := \sum_{t \in \mathcal{T}} \sum_{i \in \mathcal{I}} (r_{i,t}^* - \Delta r_{i,t}) \cdot \Delta t, \quad (18)$$

where  $f_c(\cdot)$  is the objective function of the total carbon emission rate.

Therefore, these two objective functions of the policy marker lead to a multi-objective optimization problem as

$$\min_{\pi_{\text{carbon},t}, \alpha_t, \Delta r_{i,t}, \Delta r_{k,t}} : \{ |f_n(\pi_{\text{carbon},t}, \alpha_t, \Delta r_{i,t}, \Delta r_{k,t})|, f_c(\Delta r_{i,t}) \}, \quad (19)$$

s.t.

$$\pi_{\text{carbon}}^{\min} \leq \pi_{\text{carbon},t}, \quad \forall t \in [1, |\mathcal{T}|], \quad (20)$$

$$\alpha^{\min} \leq \alpha_t, \quad \forall t \in [1, |\mathcal{T}|], \quad (21)$$

$$0 \leq \sum_{i \in \mathcal{I}} \Delta r_{i,t} \leq \sum_{i \in \mathcal{I}} r_{i,t}, \quad \forall t \in [1, |\mathcal{T}|], \quad (22)$$

where the real numbers  $\pi_{\text{carbon}}^{\min}$  and  $\alpha^{\min}$  are the fixed inputs representing the minimum levels of the carbon prices and monetary compensation rates, respectively. Equation (20) describes the constraint of carbon prices, equation (21) describes the constraint of monetary compensation rates, and equation (22) describes the constraint of targeted carbon reduction.

### 2.4. Stackelberg game-theoretic problem

In the practice of power systems, the policy maker announces the policy measures prioritizing to the responses from individual generators and consumers. The Stackelberg game-theoretic approach can precisely capture this sequential decision making process. For this reason, our research modeled the iterative negotiation between the policy maker and individual generators and consumers as a Stackelberg game. The policy maker acts as a leader with the strategies of the carbon prices and monetary compensation rates, and each of  $|\mathcal{I}|$  generators and  $|\mathcal{K}|$  consumers acts as a follower with the responding strategies of its generation, consumption and corresponding carbon emission rates. Hence, these  $(|\mathcal{I}| + |\mathcal{K}|)$  followers make decisions independently and simultaneously. As a non-cooperative game [35], the iterative negotiation between the policy maker and individual generators or consumers would reach an agreement though yielding the Stackelberg equilibrium [36], at which neither the policy maker or any generator or consumer wants to deviate. The procedure of the Stackelberg game between the leader and followers is as follows.

*Step 1:* The policy maker initializes its strategies as  $\pi_{\text{carbon},t} = \pi_{\text{carbon}}^{\min}$  and  $\alpha_t = \alpha^{\min}$ .

*Step 2:* Receiving the strategies from the policy maker, the generators and consumers decide their responding strategies through solving their optimization problems. The optimal decisions are  $\{p_{i,t}^*(\pi_{\text{carbon},t}), r_{i,t}^*(\pi_{\text{carbon},t})\}, \forall t \in [1, |\mathcal{T}|], i \in [1, |\mathcal{I}|]$ , and  $\{p_{k,t}^*(\alpha_t), r_{k,t}^*(\alpha_t)\}, \forall t \in [1, |\mathcal{T}|], k \in [1, |\mathcal{K}|]$ .

*Step 3:* After all the generators and consumers submit their responding decisions, the power system operator performs the power flow analysis under the system constraints, including the power balance constraint, voltage limits, apparent power limits, line flow limits, thermal limits, and voltage angle limits. As indicated in [37], the inputs of the power flow analysis include the active power ( $p_{i,t}^*$ ) and voltage magnitude ( $v_{i,t}$ ) of each generator belonging to the PV bus, voltage angle ( $\theta_i^{\text{ref}}$ ) and voltage magnitude ( $v_i^{\text{ref}}$ ) of the reference bus, and active power ( $p_{k,t}^*$ ) and reactive power ( $q_{k,t}$ ) of each load, i.e. PQ bus, in which  $p_{i,t}^*$  and  $p_{k,t}^*$  are obtained from the responding decisions of generators and consumers. The outputs of the power flow analysis include the reactive power ( $q_{i,t}$ ) and voltage angle ( $\theta_{i,t}$ ) of each generator belonging to the PV bus, active power ( $p_i^{\text{ref}}$ ) and reactive power ( $q_i^{\text{ref}}$ ) of the reference bus, voltage magnitude ( $v_{k,t}$ ) and voltage angle ( $\theta_{k,t}$ ) of each load, i.e. PQ bus, and power inflow ( $p_{l,t}^{\text{in}}$ ) and power outflow ( $p_{l,t}^{\text{out}}$ ) of each transmission line. Since the role of the power system operator is beyond the scope of our proposed model, for simplicity, the operation of the power flow analysis is represented by a function, denoted as  $f_{\text{pf}}(\cdot)$ , as shown in equation (23). For detailed calculation and formulation of constraints, readers can refer to [37].

$$[q_{i,t}, \theta_{i,t}, p_i^{\text{ref}}, q_i^{\text{ref}}, v_{k,t}, \theta_{k,t}, p_{l,t}^{\text{in}}, p_{l,t}^{\text{out}}] = f_{\text{pf}}(p_{i,t}^*, v_{i,t}, \theta_i^{\text{ref}}, v_i^{\text{ref}}, p_{k,t}^*, q_{k,t}), \quad (23)$$

$$\forall i \in [1, |\mathcal{I}|], k \in [1, |\mathcal{K}|], l \in [1, |\mathcal{L}|].$$

*Step 4:* Receiving the responding strategies from generators and consumers, the policy maker decides the amount of targeted carbon reduction through solving its optimization problems. The optimal decisions are  $\Delta r_{i,t}^*(p_{i,t}^*, r_{i,t}^*)$  and  $\Delta r_{k,t}^*(p_{k,t}^*, r_{k,t}^*), \forall t \in [1, |\mathcal{T}|], i \in [1, |\mathcal{I}|], k \in [1, |\mathcal{K}|]$ . Meanwhile, the policy maker updates its carbon prices and monetary compensation rates being subject to the elasticities in generation and consumption sides. The elasticity of carbon prices indicates that a change in the carbon prices would result in a change of carbon emissions incurred by generators. The elasticity of monetary compensation rates indicates that a change in the monetary compensation rates would result in a change of carbon emissions incurred by consumers. Let  $\iota$  denote the iteration number of the negotiation. The values of total carbon emissions, carbon prices, and monetary compensation rates are normalized to the value at the initial iteration, i.e.,  $\iota=1$ , as studied in [38] to define these two types of elasticities as

$$\xi_{\pi,t} := \frac{\sum_{i \in \mathcal{I}} \Delta r_{i,t} / \sum_{i \in \mathcal{I}} r_{i,t}(\iota=1)}{\Delta \pi_{\text{carbon},t} / \pi_{\text{carbon},t}(\iota=1)}, \quad \forall t \in [1, |\mathcal{T}|], \quad (24)$$

$$\xi_{\alpha,t} := \frac{\sum_{k \in \mathcal{K}} \Delta r_{k,t} / \sum_{k \in \mathcal{K}} r_{k,t}(\iota=1)}{\Delta \alpha_t / \alpha_t(\iota=1)}, \quad \forall t \in [1, |\mathcal{T}|], \quad (25)$$

where  $\xi_{\pi,t}$  and  $\xi_{\alpha,t}$  are the elasticities of the carbon price and monetary compensation rate, respectively, at the scheduling

time  $t$ . We have  $\xi_{\pi,t} < 0, \xi_{\alpha,t} < 0, \Delta r_{i,t} = r_{i,t}(\iota) - r_{i,t}(\iota+1), \Delta r_{k,t} = r_{k,t}(\iota) - r_{k,t}(\iota+1), \Delta \pi_{\text{carbon},t} = \pi_{\text{carbon},t}(\iota) - \pi_{\text{carbon},t}(\iota+1)$ , and  $\Delta \alpha_t = \alpha_t(\iota) - \alpha_t(\iota+1)$ . Hence, the carbon prices and monetary compensation rates can be updated as

$$\pi_{\text{carbon},t}(\iota+1) = \pi_{\text{carbon},t}(\iota) - \frac{\sum_{i \in \mathcal{I}} \Delta r_{i,t} \cdot \pi_{\text{carbon},t}(\iota=1)}{\xi_{\pi,t} \cdot \sum_{i \in \mathcal{I}} r_{i,t}(\iota=1)}, \quad \forall t \in [1, |\mathcal{T}|], \quad (26)$$

$$\alpha_t(\iota+1) = \alpha_t(\iota) - \frac{\sum_{k \in \mathcal{K}} \Delta r_{k,t} \cdot \alpha_t(\iota=1)}{\xi_{\alpha,t} \cdot \sum_{k \in \mathcal{K}} r_{k,t}(\iota=1)}, \quad \forall t \in [1, |\mathcal{T}|]. \quad (27)$$

*Step 5:* Receiving the updated strategies from the policy maker, generators and consumers change their responding strategies through solving their optimization problems. The iterative negotiation continues until reaching the Stackelberg equilibrium. The criteria of the Stackelberg equilibrium are the required carbon reduction drops to zero, and the carbon prices and monetary compensation rates remain unchanged as

$$\sum_{i \in \mathcal{I}} \Delta r_{i,t}^* = \sum_{k \in \mathcal{K}} \Delta r_{k,t}^* = 0, \quad \forall t \in [1, |\mathcal{T}|], \quad (28)$$

$$\pi_{\text{carbon},t}(\iota+1) = \pi_{\text{carbon},t}(\iota), \quad \forall t \in [1, |\mathcal{T}|], \quad (29)$$

$$\alpha_t(\iota+1) = \alpha_t(\iota), \quad \forall t \in [1, |\mathcal{T}|]. \quad (30)$$

The proof of how these criteria guarantee the Stackelberg equilibrium will be provided in Section 2.5. The outputs are final equilibrium solutions, denoted as  $\pi_{\text{carbon},t}^*, \alpha_t^*, p_{i,t}^*, r_{k,t}^*, p_{i,t}^*$ , and  $r_{i,t}^*$ .

The flowchart of the Stackelberg game between the leader and followers is presented in Fig. 2.

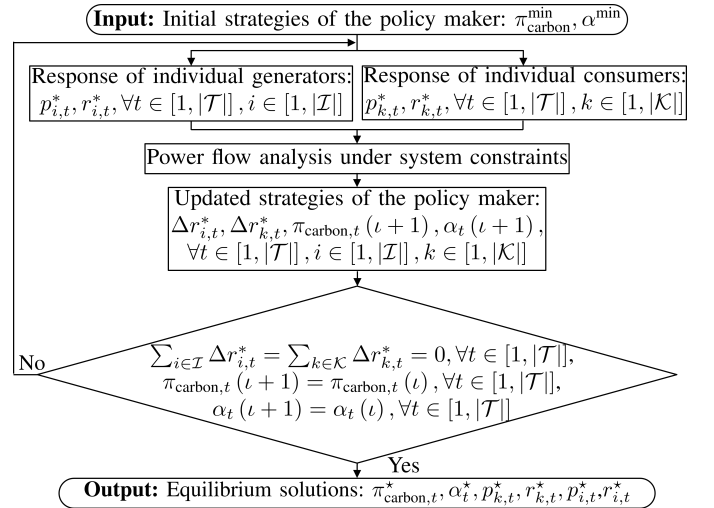


Fig. 2. Flowchart of the Stackelberg game between the leader and followers.

## 2.5. Stackelberg equilibrium

The iterative negotiation between the policy maker and generators/consumers converges to the Stackelberg equilibrium if equations (28) - (30) hold.

*Proof:* When  $\sum_{i \in \mathcal{I}} \Delta r_{i,t} > 0$ , according to (26), the carbon prices increase, i.e.,  $\pi_{\text{carbon},t}(\iota+1) > \pi_{\text{carbon},t}(\iota)$ , and when  $\sum_{k \in \mathcal{K}} \Delta r_{k,t} > 0$ , according to (27), the monetary compensation



rates increase, i.e.,  $\alpha_t(t+1) > \alpha_t(t)$ . The iterative negotiation will continue; When  $\sum_{i \in I} \Delta r_{i,t} = \sum_{k \in K} \Delta r_{k,t} = 0$ , the carbon prices and monetary compensation rates remain unchanged, i.e.,  $\pi_{\text{carbon},t}(t+1) = \pi_{\text{carbon},t}(t)$  and  $\alpha_t(t+1) = \alpha_t(t)$ . This is the point at which the iterative negotiation converges. The iterative negotiation will diverge only if  $\pi_{\text{carbon},t} < 0$  or  $\alpha_t < 0$  in any iteration. This means the  $\sum_{i \in I} \Delta r_{i,t}$  or  $\sum_{k \in K} \Delta r_{k,t}$  is negative, which violates the constraint in equation (22).

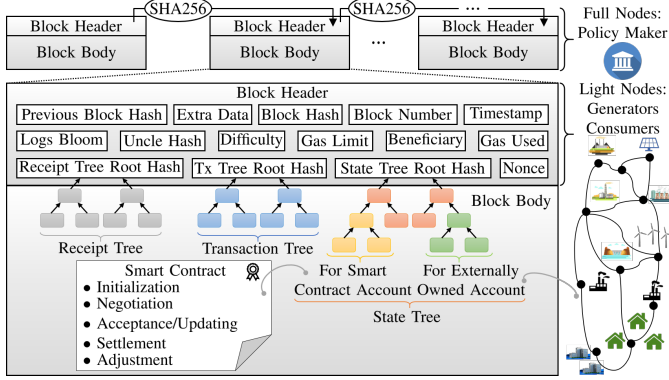


**Fig. 3.** Schematic illustration of how power system participants access to the Blockchain networks. Each block consists of the block header and block body. The full nodes (operated by the policy maker) store the information of the entire blockchain whereas the light nodes (operated by generators or consumers) only store the block header.

### 3. Blockchain for low carbon negotiation

This section introduces the data structures, node types, and smart contracts of our designed Blockchain based negotiation platform, and demonstrates the security in terms of preventing attacks to the policy maker and generators/consumers. A schematic illustration of how power system participants access to the Blockchain networks is presented in Fig. 3.

#### 3.1. Data structures

Our designed smart contracts are based on the existing Ethereum Blockchain networks [39]. As shown in Fig. 3, each block in the Blockchain consists of the block header and block body. The block body stores three types of information in the format of three modified Merkle Patricia Tries (MPTs) [39], i.e., the state tree, transaction tree, and receipt tree. The state tree contains the smart contract accounts which store codes and states of smart contracts, and the externally owned accounts which store every account's address and states, e.g., account balances. The transaction tree stores all transactions in a ledger. The receipt tree stores the outcomes of every completed transaction. The root hashes of these three MPTs and other information, e.g., the nonce and block number, are stored in the block header.

#### 3.2. Node types

The nodes of Blockchain networks are categorized as full nodes and light nodes according to the storage and computational requirements. In the context of our research as indicated

in Fig. 3, the full nodes are operated by the policy maker and the light nodes are operated by the individual generators and consumers. For the storage requirement, the full nodes store the information of every block including both the block header and block body whereas the light nodes only store the block header. For the computational requirement, the full nodes are able to mine new blocks through solving the mining puzzle [40], and need to verify all mined blocks. By contrast, the light nodes only need to verify their related transactions. The mining puzzle has the nature of 'moderately hard to solve during the block mining but easy to verify during the validation [40]'. Therefore, operating the light nodes can ease the storage and computational burdens for generators and consumers. They can easily access to the Blockchain networks by using their smart meters or smart phones.

*Remark 3:* As a permissionless Blockchain, the Ethereum Blockchain networks are open and accessible for all sectors. By operating a full node, the primary functions of the policy maker are publishing smart contracts and verifying all transactions. For this reason, the function of block mining is undertaken by the full nodes in other sectors, e.g., a mining pool or financial sector.

#### 3.3. Smart contracts

A general form of standardized functions in smart contracts is 'If an event happens, the smart contracts transfer the payments from a sender to a receiver in a self-enforcing manner'. In our research, the event is that the submitted power profiles are delivered by generators/consumers. The payments of carbon allowances are transferred from generators to the policy maker, and the payments of monetary compensations are transferred from the policy maker to consumers. Based on this general form, the negotiation procedures can be set out, by which each step is programmed as a function of smart contracts to be self-enforced. The setting out negotiation procedures of our designed smart contracts are presented in **Algorithm 1**, with details as follows:

*Step 1 (Initialization):* The policy maker calls the initialization function  $f_{\text{init}}(\cdot)$  of the smart contracts with the specified information as

$$O = f_{\text{init}}(id, \beta, \pi_{\text{carbon},t}/\alpha_t, t, \sum_{i \in I} \Delta r_{i,t} / \sum_{k \in K} \Delta r_{k,t}, t^{\text{max}}), \quad (31)$$

where  $O$  is the smart contracts initialized by the policy maker,  $id$  is the encrypted address of the policy maker,  $\beta \in \{0, 1\}$  is a binary value indicating if the policy maker contracts with generators ( $\beta=0$ ) or consumers ( $\beta=1$ ), and  $t^{\text{max}}$  is the maximum negotiation number. The Blockchain networks keep storing and updating the policy maker's contracts in the state tree.

*Step 2 (Negotiation):* Individual generators/consumers who are willing to change their power profiles for the carbon reduction call the negotiation function  $f_{\text{nego}}(\cdot)$  to enter the smart contracts, under the following conditions: 1) The maximum negotiation number is not reached, i.e.,  $t \leq t^{\text{max}}$ ; 2) The identity of a generator/consumer matches the contract type, i.e.,  $\beta_i=0$  for



**Algorithm 1** Smart contracts for low carbon negotiation

---

1: **function:** initialization  $f_{\text{init}}(\cdot)$   
2: **input:**  $id, \beta, \pi_{\text{carbon},t}, \alpha_t, t, \sum_{i \in I} \Delta r_{i,t}, \sum_{k \in K} \Delta r_{k,t}, t^{\text{max}}$   
3: **output:**  $\mathcal{O}$

---

4: **function:** negotiation  $f_{\text{nego}}(\cdot)$   
5: **input:**  $\iota, \beta_i, \beta_k, p_{i,t}^*, p_{k,t}^*, r_{i,t}^*, r_{k,t}^*, p_i^{\min}, p_k^{\min}, p_i^{\max}, p_k^{\max}$   
6: **require:**  $\iota \leq t^{\text{max}}, \beta_i=0, \beta_k=1$   
7:   log the negotiation event  
8: **output:**  $\mathcal{E}$

---

9: **function:** acceptance/updating  $f_{\text{update}}(\cdot)$   
10: **input:**  $\pi_{\text{carbon},t}(\iota), \alpha_t(\iota)$   
11:   accept satisfied generators/consumers and update carbon prices/monetary compensation rates  
12: **output:**  $\pi_{\text{carbon},t}(\iota + 1), \alpha_t(\iota + 1)$

---

13: **function:** settlement  $f_{\text{pay}}(\cdot)$   
14: **input:**  $t_{\text{now}}, r_{i,t}, r_{k,t}, c_{\text{carbon},i}, \gamma_k$   
15: **require:**  $t_{\text{now}} > t, r_{i,t} = r_{i,t}^*, r_{k,t} = r_{k,t}^*$   
16:   transfer the payments to receivers  
17: **output:**  $b, b_i, b_k$

---

18: **function:** adjustment  $f_{\text{adjust}}(\cdot)$   
19: **input:**  $t_{\text{now}}, r_{i,t}, r_{k,t}, r_{i,t}^*, r_{k,t}^*, c_{\text{carbon},i}, \gamma_k$   
20: **require:**  $t_{\text{now}} > t, r_{i,t} \neq r_{i,t}^*, r_{k,t} \neq r_{k,t}^*$   
21:   withdraw or repay according to the actual delivery  
22: **output:**  $b, b_i$

---

the generator  $i$ , or  $\beta_k=1$  for the consumer  $k$ . Once a generator/consumer successfully enters smart contracts, an event is logged in the ledger containing the negotiating information as

$$\mathcal{E} = f_{\text{nego}}(\iota, \beta_i/\beta_k, p_{i,t}^*/p_{k,t}^*, r_{i,t}^*/r_{k,t}^*, p_i^{\min}/p_k^{\min}, p_i^{\max}/p_k^{\max}), \quad (32)$$

where  $\mathcal{E}$  is the event stored in the ledger. The optimal power profiles and corresponding carbon emission rates are external inputs to smart contracts yielded by solving optimization problems of generators/consumers.

*Step 3 (Acceptance/Updating):* The policy maker accepts the submitted power profiles which satisfy the targeted carbon reduction. The payments of carbon allowances are deducted from accounts of generators, and the payments of monetary compensations are deducted from the account of the policy maker.

For other unsatisfied power profiles, the policy maker declines them and calls the update function  $f_{\text{update}}(\cdot)$  to update the carbon prices or monetary compensation rates according to equations (26) or (27), respectively. The declined generators/consumers can resubmit their power profiles yielded by solving their optimization problems with updated carbon prices/monetary compensation rates. This step continues until the policy maker comes to an agreement with all generators and consumers, or the maximum iteration number is reached, i.e.,  $\iota = t^{\text{max}}$ .

*Step 4 (Settlement):* After the actual operation, i.e.,  $t_{\text{now}} > t$ , where  $t_{\text{now}}$  is the current time, the smart contracts query smart meters or sensors to confirm the delivery of power profiles. For the delivered power profiles, the deducted payments are trans-

ferred to accounts of receivers by the pay function  $f_{\text{pay}}(\cdot)$  as

$$b_i = f_{\text{pay}}(t_{\text{now}}, r_{i,t}, c_{\text{carbon},i}), \quad (33)$$

$$b_k = f_{\text{pay}}(t_{\text{now}}, r_{k,t}, \gamma_k), \quad (34)$$

$$b = f_{\text{pay}}(t_{\text{now}}, r_{i,t}, r_{k,t}, c_{\text{carbon},i}, \gamma_k), \quad (35)$$

where  $b$ ,  $b_i$ , and  $b_k$  are the updated account balances of the policy maker, generator  $i$ , and consumer  $k$ , respectively, after receiving the transferred payments from the smart contracts. We have  $b_i = \bar{b}_i - c_{\text{carbon},i}(r_{i,t})$ ,  $b_k = \bar{b}_k + \gamma_k(r_{k,t})$ , and  $b = \bar{b} + \sum_{i \in I} c_{\text{carbon},i}(r_{i,t}) - \sum_{k \in K} \gamma_k(r_{k,t})$ , where  $\bar{b}$ ,  $\bar{b}_i$ , and  $\bar{b}_k$  are the corresponding original account balances.

*Step 5 (Adjustment):* For the under delivered consumers, i.e.,  $r_{k,t} > r_{k,t}^*$ , and over delivered generators, i.e.,  $r_{i,t} < r_{i,t}^*$ , they need to send a notice to the policy maker. Then, the policy maker and these generators can call the adjustment function  $f_{\text{adjust}}(\cdot)$  to withdraw their over deposited monetary compensations and carbon costs, respectively, as

$$b = f_{\text{adjust}}(t_{\text{now}}, r_{k,t}^*, r_{k,t}, \gamma_k), \quad (36)$$

$$b_i = f_{\text{adjust}}(t_{\text{now}}, r_{i,t}^*, r_{i,t}, c_{\text{carbon},i}), \quad (37)$$

where  $b = \bar{b} + \gamma_k(r_{k,t}^*) - \gamma_k(r_{k,t})$  and  $b_i = \bar{b}_i + c_{\text{carbon},i}(r_{i,t}^*) - c_{\text{carbon},i}(r_{i,t})$ .

For the over delivered consumers, i.e.,  $r_{k,t} < r_{k,t}^*$ , and under delivered generators, i.e.,  $r_{i,t} > r_{i,t}^*$ , they also need to send a notice to the policy maker. The smart contracts will automatically deduct the extra monetary compensations and carbon costs from the accounts of the policy maker and these generators, respectively. Then, they need to call the same adjustment function to repay these deductions as  $b = \bar{b} - [\gamma_k(r_{k,t}) - \gamma_k(r_{k,t}^*)]$  and  $b_i = \bar{b}_i - [c_{\text{carbon},i}(r_{i,t}) - c_{\text{carbon},i}(r_{i,t}^*)]$ .

### 3.4. Preventing attacks

A malicious node would attempt to attack the proposed negotiation platform from 1) smart contracts initialized the policy maker to alter carbon prices and monetary compensation rates, and 2) meter readings of generators/consumers to alter power profiles and carbon emission rates. The consequences of these attacks and how the Blockchain networks can prevent these attacks are discussed as follows.

#### 3.4.1. Attacks to the policy maker

When a malicious node alters the carbon price from  $\pi_{\text{carbon},t}$  to  $\pi_{\text{carbon},t}^{\text{tamper}} = \pi_{\text{carbon},t} - \Delta\pi_{\text{carbon},t}$ , according to equation (24), the carbon emission rate becomes

$$\sum_{i \in I} r_{i,t}^{\text{tamper}} = \sum_{i \in I} r_{i,t} - \frac{\xi \pi_{i,t} \cdot \sum_{i \in I} r_{i,t}(\iota = 1) \cdot \Delta\pi_{\text{carbon},t}}{\pi_{\text{carbon},t}(\iota = 1)}. \quad (38)$$

This indicates that the total carbon emission rate will increase if  $\Delta\pi_{\text{carbon},t} > 0$ , i.e.,  $\pi_{\text{carbon},t}^{\text{tamper}} < \pi_{\text{carbon},t}$ , and decrease if  $\Delta\pi_{\text{carbon},t} < 0$ , i.e.,  $\pi_{\text{carbon},t}^{\text{tamper}} > \pi_{\text{carbon},t}$ . This is the same case when a malicious node alters the monetary compensation rate. Thus, if a malicious node attacks the policy maker by increasing carbon prices or monetary compensation rates above the point at which the maximum level of the carbon reduction is reached, i.e.,

$\sum_{i \in I} \Delta r_{i,t} = \sum_{k \in K} \Delta r_{k,t} = 0$ , it would cause an additional financial loss for the policy maker; If a malicious node attacks the policy maker by decreasing the carbon prices or monetary compensation rates below the point at which the maximum level of the carbon reduction is reached, the policy maker would fail to achieve its targeted carbon reduction.

The Blockchain networks can protect the policy maker from this attack, since the carbon prices and monetary compensation rates are recorded in the smart contract account of the state tree. The only way to alter the smart contracts is to mine a new block with the tampered states of the smart contract account. This new block needs to be verified by all full nodes including the policy maker itself. If the signature of the tampered smart contracts does not match the policy maker's identity, the new block would fail to be verified by a majority of full nodes.

### 3.4.2. Attacks to generators/consumers

When a malicious node alters the meter reading of a generator from  $r_{i,t}$  to  $r_{i,t}^{\text{tamper}} = r_{i,t} - \Delta r_{i,t}$ , according to equation (4), the carbon cost of this generator becomes

$$c_{\text{carbon},i}(r_{i,t}^{\text{tamper}}) = r_{i,t} \cdot \Delta t \cdot \pi_{\text{carbon},t} - \Delta r_{i,t} \cdot \Delta t \cdot \pi_{\text{carbon},t}. \quad (39)$$

This indicates that the carbon cost will increase if  $\Delta r_{i,t} < 0$ , i.e.,  $r_{i,t}^{\text{tamper}} > r_{i,t}$ , and decrease if  $\Delta r_{i,t} > 0$ , i.e.,  $r_{i,t}^{\text{tamper}} < r_{i,t}$ . Therefore, if a malicious node attacks a generator by increasing the meter reading of the carbon emission rate, the carbon cost of this generator would be overcharged; If a malicious node attacks a generator by decreasing the meter reading of the carbon emission rate, the extra carbon emissions would not be repaid by this generator in the monetary manner.

When a malicious node alters the meter reading of a consumer from  $r_{k,t}$  to  $r_{k,t}^{\text{tamper}} = r_{k,t} - \Delta r_{k,t}$ , according to equation (14), the monetary compensation of this consumer becomes

$$\gamma_k(r_{k,t}^{\text{tamper}}, \bar{r}_{k,t}) = \begin{cases} \alpha_t \cdot \sqrt{(\bar{r}_{k,t} \cdot \Delta t)^2 - [(r_{k,t} - \Delta r_{k,t}) \cdot \Delta t]^2}, & \bar{r}_{k,t} > r_{k,t}^{\text{tamper}}, \\ 0, & \bar{r}_{k,t} \leq r_{k,t}^{\text{tamper}}. \end{cases} \quad (40)$$

This indicates that the monetary compensation will increase if  $\Delta r_{k,t} > 0$ , i.e.,  $r_{k,t}^{\text{tamper}} < r_{k,t}$ , and decrease if  $\Delta r_{k,t} < 0$ , i.e.,  $r_{k,t}^{\text{tamper}} > r_{k,t}$ , until  $r_{k,t}^{\text{tamper}} \geq \bar{r}_{k,t}$  after which this consumer will not receive any monetary compensation. Therefore, if a malicious node attacks a consumer by increasing the meter reading of the carbon emission rate, the consumer would receive less monetary compensation than the amount that repays its carbon reduction; If a malicious node attacks a consumer by decreasing the meter reading of the carbon emission rate, it would cause an additional financial loss for the policy maker due to the extra monetary compensation.

The blockchain networks can protect the generators/consumers from this attack. If a malicious node alters the meter reading of any generator/consumer, this attack would be sensed by every node, since the tampered meter reading does not match the submitted amount of the carbon emission rate recorded in the blockchain networks, and there is no notice of the over or under delivery. After this attack is sensed, the

policy maker can calculate the actual carbon emission rate of this generator/consumer according to the carbon emission conservation in equation (15) and the meter readings of other generators/consumers. Then, the policy maker and attacked generator/consumer can call the adjustment function in smart contracts to amend payments.

*Remark 4:* In addition to these attacks on stakeholders in power systems, there are common attacks on the Blockchain networks, e.g., the double spending attack and Goldfinger attack [41], which can be managed by the Ethereum Blockchain networks. For the double spending attack, since the Ethereum Blockchain is an account based ledger, which means that the amount of transferred currency would be directly deducted from the account balance of the sender (even if a malicious sender falsifies a transaction), the double spending attack can be naturally prevented. To prevent the Goldfinger attack, the Ethereum is transitioning towards the consensus of the proof of stake [42], in which miners are randomly selected to validate transactions and mine blocks based on their stakes in the networks. This can prevent a malicious node with strong computational power to manipulate the Blockchain networks.

## 4. Case studies

Case studies have been conducted to evaluate the proposed model in the context of the GB power systems and energy markets. The simulations are performed by a machine with the Intel<sup>®</sup> Core<sup>™</sup> i9-9900K CPU at 3.60 GHz. The proposed algorithm for the power system scheduling is written in the MATLAB language. The Stackelberg game-theoretic problem is solved by the artificial immune algorithm as detailed in [24]. The proposed smart contracts are written in the Solidity language and executed on the Remix-IDE.

The GB 29-bus test system is adopted by our research as shown in Fig. 4 to represent the technical properties of the GB transmission networks whilst reducing the complexity. This system consists of 29 buses, 98 double-circuit branches, 1 single-circuit branch, and 89 generators. The total installed capacity of each generation source is allocated to this system according to the installed capacities and locations of the GB power plants at the end of 2020 [43]. The real-time GB power consumption is obtained from the GridWatch [44]. The average retail and wholesale electricity prices in the GB energy markets [45] are adopted as  $\pi_r = £144/\text{MWh}$  and  $\pi_{\text{ws},t} = £65/\text{MWh}$ , respectively, under the flat electricity pricing to specifically investigate the impacts of the carbon prices and monetary compensation rates. The coefficients of operating costs for the projects commissioning in 2020 [31] are adopted. The GB carbon price support is used as  $\pi_{\text{carbon},t}^{\text{min}} = £18/\text{ton}$ . The proposed model is compared with the following two cases to evaluate the performances:

- *Case 1 (Benchmark):* The benchmark is yielded by the sum of the GB power system historical data of four representative days in 2020 [44] with equal weight. The GB carbon price support plus the prices from the EU emissions trading scheme is used as the carbon prices and there is no monetary compensation.

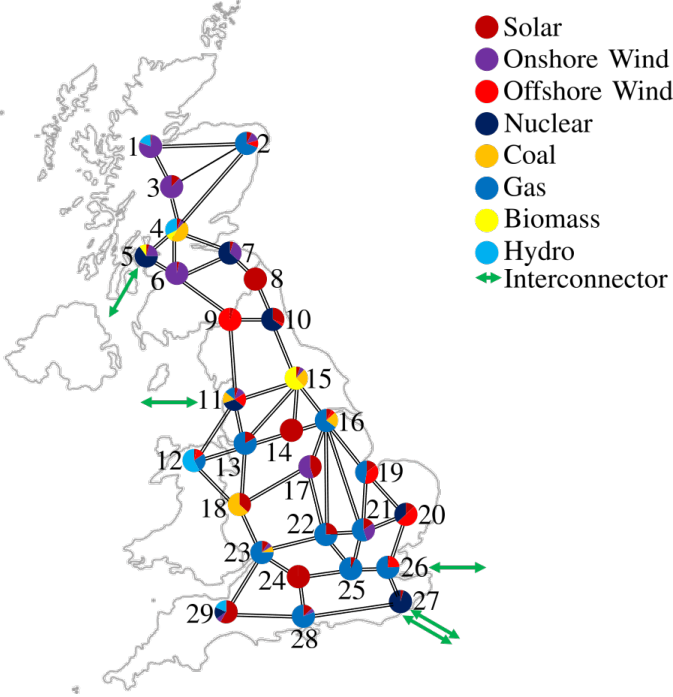


**Fig. 4.** Schematic illustration of the GB 29-bus test system and allocation of generation capacities. The percentages of allocated capacities are shown in the pie chart of each bus.

- **Case 2 (Non-negotiation):** As proposed in [24], the policy maker and generators/consumers decide their strategies simultaneously without the iterative negotiation, forming a multi-objective optimization problem.

#### 4.1. Scheduling performances

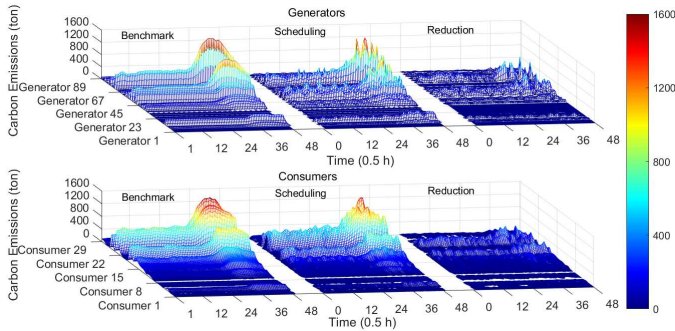


**Fig. 5.** Carbon emissions tracing for generators/consumers over the scheduling process. The  $x$  axes indicate the scheduling time of a day. The  $y$  axes indicate the number of generators/consumers. The  $z$  axes and colorbar indicate the carbon emissions of individual generators/consumers for a given 0.5 h scheduling interval. ‘Benchmark’ and ‘Scheduling’ refer to the carbon emissions before and after the scheduling, respectively. ‘Reduction’ refers to the difference of carbon emissions before and after the scheduling.

The carbon emissions tracing for individual generators/consumers over the scheduling process is presented in Fig. 5. The carbon emissions from the high-carbon generators/consumers are reduced during every scheduling interval. For the generation side as shown at the top of Fig. 5, during

the peak demand period from the twenty-fifth scheduling time to the thirty-sixth scheduling time, about 500 tons of carbon emissions per half-hour are reduced, accounting for 31.25% of the highest carbon emission rate from generators. This is because the fossil fuel based generators, e.g., the coal and gas generators, are incentivized to ramp down their power outputs in avoiding the high carbon costs. To complement the decrease of coal and gas for meeting the demand, the daily percentage of renewable energy sources increases from 39.53% at the benchmark to 45.13% after the scheduling. For the consumption side as shown at the bottom of Fig. 5, during the peak demand period, about 200 tons of carbon emissions per half-hour are reduced, accounting for 13.33% of the highest carbon emission rate from consumers. This is because consumers in high carbon time and location are incentivized to shift away/curtail their demand for earning the monetary compensations.

##### 4.1.1. Impacts of carbon prices on generators

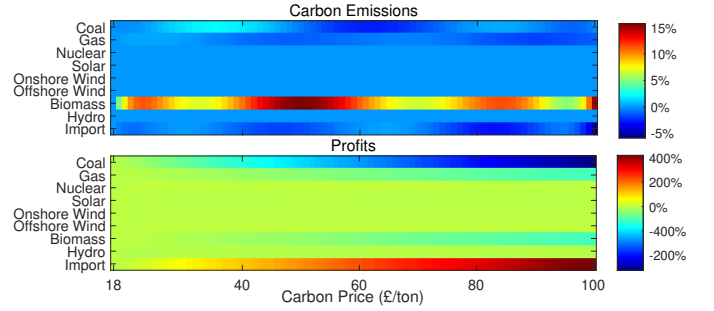


**Fig. 6.** Carbon emissions and profits of generators as a function of carbon prices. Generators with the same source are aggregated. The  $x$  axes indicate the carbon prices. The  $y$  axes indicate the generation sources. The colorbars indicate the percentage of increase (positive)/decrease (negative) of carbon emissions and profits for each source at a given carbon price, compared to the benchmark carbon emissions and profits.

The chromatograms in Fig. 6 show the trends of carbon emissions and profits of various generation sources as the carbon prices increase. For the carbon emissions as shown at the top of Fig. 6, with the increase of carbon prices, the coal and gas generators are incentivized to ramp down for saving costs. It is noted that the carbon emissions from the coal generation increase when the carbon prices rise from £28/ton to £42/ton. The reason is that when only a marginal portion of coal generation is replaced by renewable generation, the slight carbon reduction would be offset by the increased carbon emission intensity due to the part-load operation of coal generators. For the profits as shown at the bottom of Fig. 6, the generating profits of coal, gas, and biomass decrease with the increase of the carbon prices. When the carbon prices exceed £33/ton and £92/ton, the generating profits of coal and gas would drop to negative, respectively. This is because the revenues of these generators are offset by the generating costs and increased carbon costs. The profits of the power import increase with the rise of carbon prices, because the carbon prices of other regions are assumed to keep unchanged at the benchmark price and become lower than the local carbon prices.

#### 4.1.2. Impacts of monetary compensation rates on consumers

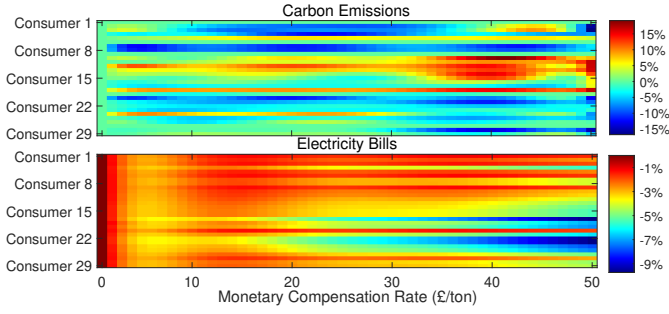


**Fig. 7.** Carbon emissions and electricity bills of consumers as a function of monetary compensation rates. The  $x$  axes indicate the monetary compensation rates. The  $y$  axes indicate the number of consumers. The colorbars indicate the percentage of increase (positive)/decrease (negative) of carbon emissions and electricity bills for each consumer at a given monetary compensation rate, compared to the benchmark carbon emissions and electricity bills.

The chromatograms in Fig. 7 show the trends of carbon emissions and electricity bills of consumers as the monetary compensation rates increase. For the carbon emissions as shown at the top of Fig. 7, the consumers at low carbon locations, i.e., the consumers 10-15, would not be significantly affected by the monetary compensation. By contrast, the consumers at high carbon locations, i.e., the rest consumers, would receive more monetary compensations, and therefore curtail or shift away their loads for saving bills. For the electricity bills as shown at the bottom of Fig. 7, the bills of consumers gradually decrease with the increase of the monetary compensation rates. When the monetary compensation rates exceed £33/ton, approximately 9% of electricity bills are saved for consumers at high carbon locations through 10% of the carbon reduction.

#### 4.2. Negotiation performances

The comparison of objective functions is presented in Table 1. The electricity bills of all consumers and profits of all generators are aggregated for comparisons. Our proposed model yields the lowest carbon emissions in comparison to the aforementioned benchmark and non-negotiation cases. This is because our proposed model provides generators and consumers with an opportunity to iteratively negotiate until the maximum potential of the carbon reduction is reached at the Stackelberg equilibrium. By contrast, the non-negotiation case only allows a single round of the interaction between the policy maker and generators/consumers, even though they have the potential and willingness to further change their power profiles for the carbon reduction. For daily profits, our proposed model can improve the profits of renewable generators whereas reduce the profits of fossil fuel based generators. Since these fossil fuel based generators account for a majority of the generation capacity, the total profits of our proposed model are the lowest.

#### 4.3. Demonstration of executing smart contracts

The demonstration of executing our designed smart contracts is presented in Fig. 8 to show how the smart contracts interact with the participants of power systems. Two generators and

**Table 1** Comparison of yielded objective functions.

	Benchmark	Proposed Model	Non-negotiation
Daily Carbon Emissions (kton)	42.92	37.15	38.63
Daily Electricity Bills (m£)	105.51	95.96	96.97
Daily Profits (m£)	17.92	16.58	16.68

two consumers are selected as examples, of which generator 1 and 2 use the coal and gas, respectively. The policy maker calls the initialization function from the blockchain networks to specify the contract conditions. The generators and consumers subsequently call the negotiation function to submit their power profiles and incurred carbon emission rates. Fig. 8 samples the negotiation at the twenty-third iteration. At this iteration, the policy maker accepts the submissions of generator 1, consumer 1, and consumer 2, whereas declines the submission of generator 2 and then increases the carbon prices. After receiving the delivery signals from generators and consumers, the smart contracts pay the deposited carbon costs and monetary compensations to the policy maker and consumer 1, respectively. Since the consumer 2's actual carbon emission rate exceeds the submitted carbon emission rate and is larger than the carbon emission rate in the previous iteration, the policy maker calls the adjusting function to withdraw all the deposited monetary compensation for consumer 2.

#### 5. Conclusion

This paper proposed a consumer-centric and Blockchain-based framework for enabling decarbonization and automated negotiations between the policy maker and consumers/generators. The process of the strategic negotiation was modeled as a Stackelberg game-theoretic problem, and the agreement was reached by finding the Stackelberg equilibrium. The setting out negotiating procedures were executed and self-enforced by designed Blockchain based smart contracts. The states, transactions, and receipts of the negotiation were structured as the MPTs for reducing the information burdens. Operating the light nodes allowed both consumers and generators to participant in the negotiation with lower computational and storage requirements. The consequences of potential cyber attacks to smart contracts and meter readings, and how Blockchain networks can prevent these attacks were also investigated. Case studies show that the proposed framework was capable of improving the percentage of renewable energy generation by 45.13%, saving 9% bills for consumers, and reducing over 40% of carbon emissions in total. As a future work, because individual consumers could have idiosyncratic preferences, e.g., particular bill saving target or convenience requirements, we will develop more scalable frameworks to capture these preferences with diverse parameters and objective functions.

#### Appendix A. Carbon emissions tracing

Consider a power network with  $|N|$  buses,  $|I|$  generators,  $|K|$  loads, and  $|L|$  transmission lines, under which the carbon emis-

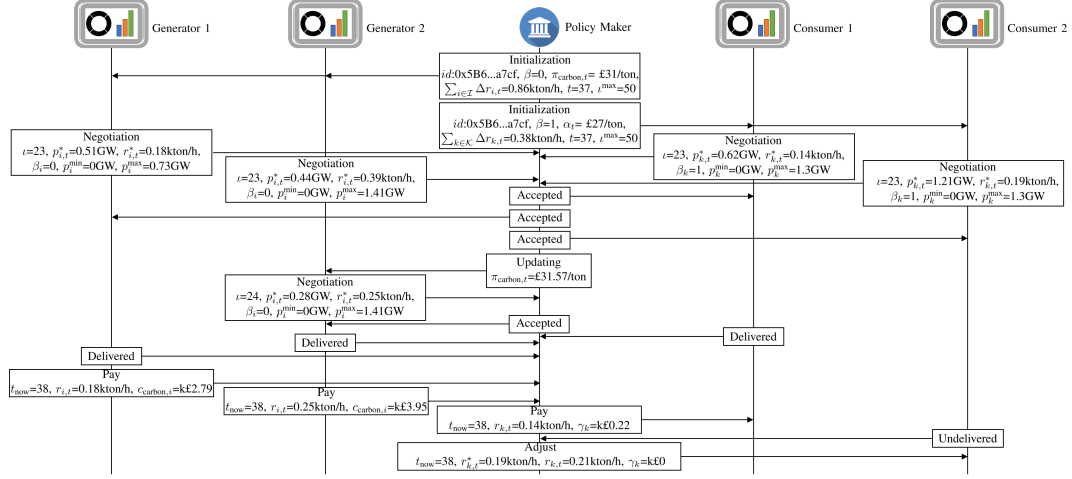


Fig. 8. Demonstration of executing smart contracts for low carbon negotiation.

sions flow (CEF) is categorized as the CEF from the generation (CEFG), the CEF from the transmission (CEFT), the CEF from the transmission loss (CEFL), and the CEF from the consumption (CEFC).

#### Appendix A.1. Carbon emissions flow from the generation

The CEFG traces the carbon emissions caused by the electricity generation due to the combustion of fossil fuels. The carbon emission intensities of generators are determined by the carbon emission intensities of input fuels and efficiency of the electricity supply [29]. Let an  $|I|$ -size column vector  $\mathbf{e}_{\text{CEFG}}$  denote the carbon emission intensities of generators. The carbon emission rates of generators can be calculated as

$$\mathbf{r}_{\text{CEFG}} = \mathbf{P}_{\text{CEFG}} \times \mathbf{e}_{\text{CEFG}}, \quad (\text{A.1})$$

where  $\mathbf{r}_{\text{CEFG}}$  is a  $|N|$ -size column vector to denote the carbon emission rates of generators, and  $\mathbf{P}_{\text{CEFG}}$  is a  $(|N|, |I|)$ -size matrix to denote the power outputs of generators. The indices  $n$  and  $i$  of each element  $p_{\text{CEFG},n,i} \in \mathbf{P}_{\text{CEFG}}$  indicate that the generator  $i$  is located at the bus  $n$ . For the buses without generators, the corresponding elements equal to zero.

#### Appendix A.2. Carbon emissions flows from the transmission and consumption

The CEFT and CEFC trace the carbon emissions caused by generators when the electricity is transmitted and consumed, respectively. Firstly, to calculate the carbon emission rates of the transmission and consumption, the corresponding carbon emission intensities need to be analyzed. According to the proportional sharing principle [46] and distribution of the CEF [32], the following two properties hold for the distribution of the CEFT and CEFC. A schematic illustration of these two properties is presented in Fig. A.9.

- *Property 1*: The CEF caused by all power outflows from a bus (including the power outflows to the loads connected to this bus) equals to the CEF caused by all power inflows to this bus (including the power inflows from the generators connected to this bus).

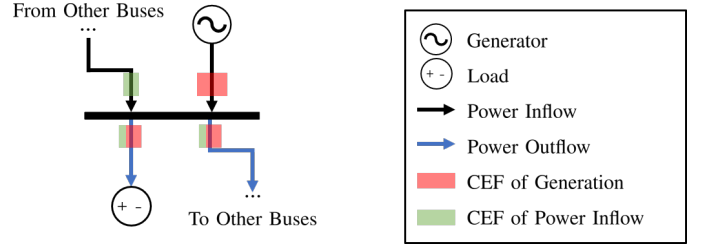


Fig. A.9. Schematic illustration for the distribution of the CEFT and CEFC. The CEF caused by all power outflows from a bus equals to the CEF caused by all power inflows to this bus (indicated by the size of the CEF box). The bus homogenizes the carbon emission intensities of all power inflows (indicated by the color of the CEF box), so that all power outflows have the same carbon emission intensities.

- *Property 2*: The proportion of the CEF caused by one power inflow to the CEF caused by all power inflows keeps unchanged in the CEFs caused by each power outflow. Hence, all power outflows from the same bus would have the same carbon emission intensities.

Let a  $(|N|, |N|)$ -size square matrix  $\mathbf{P}_B$  denote the distribution of the power inflows from other buses yielded by the power flow analysis. The indices  $n_a$  and  $n_b$  ( $n_a, n_b \in N$ ) of each element  $p_{B,n_a,n_b} \in \mathbf{P}_B$  indicate the direction of the power inflow in the transmission line is from the bus  $n_a$  to the bus  $n_b$ . Recall that  $\mathbf{P}_{\text{CEFG}}$  represents the power inflows from generators. The distribution of power inflows from both other buses and generators can be described as

$$\mathbf{P}_{\text{CEFT}} = \text{diag} \left\{ \mathbf{i}_{(|N|+|I|)} \times \begin{bmatrix} \mathbf{P}_B \\ \mathbf{P}_{\text{CEFG}}^T \end{bmatrix} \right\}, \quad (\text{A.2})$$

where  $\mathbf{P}_{\text{CEFT}}$  is a  $(|N|, |N|)$ -size diagonal matrix to denote the distribution of the total power inflows from both other buses and generators,  $\text{diag} \{\cdot\}$  is the operation to create the diagonal matrix, and  $\mathbf{i}_{(|N|+|I|)}$  is a  $(|N| + |I|)$ -size unit row vector.

According to the *Property 1*, the carbon emission rates caused by all power inflows to each of buses equal to the carbon emission rates caused by all power inflows from other buses and

generators as

$$\mathbf{P}_{\text{CEFT}} \times \mathbf{e}_{\text{CEFT}} = \mathbf{P}_{\text{B}}^{\text{T}} \times \mathbf{e}_{\text{CEFT}} + \mathbf{R}_{\text{CEFG}}, \quad (\text{A.3})$$

where  $\mathbf{e}_{\text{CEFT}}$  is a  $|\mathcal{N}|$ -size column vector to denote the carbon emission intensities of the transmission and consumption. From the equation (A.3), we have

$$\mathbf{e}_{\text{CEFT}} = (\mathbf{P}_{\text{CEFT}} - \mathbf{P}_{\text{B}}^{\text{T}})^{-1} \times \mathbf{R}_{\text{CEFG}}. \quad (\text{A.4})$$

Secondly, the carbon emission rates of the transmission and consumption can be calculated as

$$\mathbf{R}_{\text{CEFT}} = \text{diag}\{\mathbf{e}_{\text{CEFT}}\} \times \mathbf{P}_{\text{B}}, \quad (\text{A.5})$$

$$\mathbf{R}_{\text{CEFC}} = \text{diag}\{\mathbf{e}_{\text{CEFT}}\} \times \mathbf{P}_{\text{CEFC}}, \quad (\text{A.6})$$

where  $\mathbf{R}_{\text{CEFT}}$  is a  $(|\mathcal{N}|, |\mathcal{N}|)$ -size square matrix to denote the carbon emission rates of the transmission,  $\mathbf{R}_{\text{CEFC}}$  is a  $(|\mathcal{N}|, |\mathcal{K}|)$ -size matrix to denote the carbon emission rates of the consumption, and  $\mathbf{P}_{\text{CEFC}}$  is a  $(|\mathcal{N}|, |\mathcal{K}|)$ -size matrix to denote the distribution of power loads. The indices  $n_a$  and  $n_b$  ( $n_a, n_b \in \mathcal{N}$ ) of each element  $r_{\text{CEFT}, n_a, n_b} \in \mathbf{R}_{\text{CEFT}}$  indicate the direction of the CEFT in the transmission line is from the bus  $n_a$  to the bus  $n_b$ . The indices  $n$  and  $k$  of elements  $r_{\text{CEFC}, n, k} \in \mathbf{R}_{\text{CEFC}}$  and  $p_{\text{CEFC}, n, k} \in \mathbf{P}_{\text{CEFC}}$  indicate that the load  $k$  is located at the bus  $n$ .

#### Appendix A.3. Carbon emissions flow from the transmission loss

According to the *Property 2*, the power loss can be taken as a power outflow from a bus, and has the same carbon emission intensities with other power outflows from this bus. Recall that  $\mathbf{P}_{\text{B}}$  denotes the distribution of power inflows to each of buses in power networks. Let a  $(|\mathcal{N}|, |\mathcal{N}|)$ -size square matrix  $\mathbf{P}'_{\text{B}}$  denote the distribution of power outflows from each of buses in power networks. The carbon emission rates of transmission losses can be calculated as

$$\mathbf{R}_{\text{CEFL}} = \text{diag}\{\mathbf{e}_{\text{CEFT}}\} \times (\mathbf{P}'_{\text{B}} - \mathbf{P}_{\text{B}}), \quad (\text{A.7})$$

where  $\mathbf{R}_{\text{CEFL}}$  is a  $(|\mathcal{N}|, |\mathcal{N}|)$ -size square matrix to denote the carbon emission rates of transmission losses. The indices  $n_a$  and  $n_b$  ( $n_a, n_b \in \mathcal{N}$ ) of each element  $r_{\text{CEFL}, n_a, n_b} \in \mathbf{R}_{\text{CEFL}}$  indicate the direction of the CEFL in the transmission line is from the bus  $n_a$  to the bus  $n_b$ .

### Appendix B. Solution to the Stackelberg game-theoretic problem

#### Appendix B.1. Problem analysis

Using the equality constraints in equations (5) and (13), the followers' decision variables  $r_{i,t}$  and  $r_{k,t}$  can be substituted by  $p_{i,t}$  and  $p_{k,t}$ , respectively. Using the equality constraint in equation (16), the leader's decision variable  $\Delta r_{k,t}$  can be substituted by  $\Delta r_{i,t}$ . These equality constraints can be subsequently eliminated. First, the decision variables and objective functions of the established problem can be described in the following vector-valued manner to facilitate the discussions of the solution.

$$\mathbf{p}_{\text{follower}} = [p_{i,t}, p_{k,t}], \forall t \in [1, |\mathcal{T}|], i \in [1, |\mathcal{I}|], k \in [1, |\mathcal{K}|], \quad (\text{B.1})$$

$$\mathbf{p}_{\text{leader}} = [\Delta r_{k,t}], \forall t \in [1, |\mathcal{T}|], k \in [1, |\mathcal{K}|], \quad (\text{B.2})$$

$$\mathbf{f}_{\text{leader}} = [f_n(\pi_{\text{carbon},t}, \alpha_t, \Delta r_{i,t}), f_c(\Delta r_{i,t})], \quad (\text{B.3})$$

$$\mathbf{f}_{\text{follower}} = [-f_i(p_{i,t}), f_k(p_{k,t})], \forall i \in [1, |\mathcal{I}|], k \in [1, |\mathcal{K}|], \quad (\text{B.4})$$

where  $\mathbf{p}_{\text{follower}}$  is a row vector to denote the decision variables of followers,  $\mathbf{p}_{\text{leader}}$  is a row vector to denote the decision variables of the leader,  $\mathbf{f}_{\text{follower}}$  is a row vector to denote the objective functions of followers, and  $\mathbf{f}_{\text{leader}}$  is a row vector to denote the objective functions of the leader. Additionally, the lower bounds and upper bounds of the decision variables of followers in equations (2) and (12) are denoted by vectors  $\underline{\mathbf{p}}_{\text{follower}}$  and  $\bar{\mathbf{p}}_{\text{follower}}$ , respectively. The lower bounds and upper bounds of the decision variables of the leader in equations (20) - (22) are denoted by vectors  $\underline{\mathbf{p}}_{\text{leader}}$  and  $\bar{\mathbf{p}}_{\text{leader}}$ , respectively.

Next, the solution of the Stackelberg game-theoretic problem is analyzed. For simplicity, in the equation (14), we only consider the case that the consumer can receive the monetary compensation, i.e.,  $\bar{r}_{k,t} > r_{k,t}$ , and the equation (13) is denoted as  $r_{k,t} = p_{k,t} \cdot A$ . Using the Lagrange's multipliers  $\lambda_1$  and  $\lambda_2$  for the constraint (12), the constrained optimization problem can be converted to the following form

$$L(p_{k,t}, \lambda_1, \lambda_2) = \sum_{t \in \mathcal{T}} \left[ p_{k,t} \cdot \Delta t \cdot \pi_t - \alpha_t \cdot \sqrt{(\bar{r}_{k,t} \cdot \Delta t)^2 - (A \cdot p_{k,t} \cdot \Delta t)^2} \right] + \lambda_1 (p_k^{\min} - p_{k,t}) + \lambda_2 (p_{k,t} - p_k^{\max}). \quad (\text{B.5})$$

The corresponding KKT conditions are as follows:

$$\frac{\partial L}{\partial p_{k,t}} = \Delta t \cdot \pi_t + \alpha_t \cdot \frac{(A \cdot p_{k,t} \cdot \Delta t) \cdot (A \cdot \Delta t)}{\sqrt{(\bar{r}_{k,t} \cdot \Delta t)^2 - (A \cdot p_{k,t} \cdot \Delta t)^2}} - \lambda_1 + \lambda_2, \quad (\text{B.6})$$

$$\lambda_1 (p_k^{\min} - p_{k,t}) = 0, \quad (\text{B.7})$$

$$\lambda_2 (p_{k,t} - p_k^{\max}) = 0, \quad (\text{B.8})$$

$$\lambda_1, \lambda_2 \geq 0. \quad (\text{B.9})$$

When  $p_{k,t} = p_k^{\min}$ , i.e.,  $p_{k,t} < p_k^{\max}$ . From (B.8), we have  $\lambda_2 = 0$ . From (B.6), we have

$$\lambda_1 = \Delta t \cdot \pi_t + \alpha_t \cdot \frac{(A \cdot p_k^{\min} \cdot \Delta t) \cdot (A \cdot \Delta t)}{\sqrt{(\bar{r}_{k,t} \cdot \Delta t)^2 - (A \cdot p_k^{\min} \cdot \Delta t)^2}} > 0. \quad (\text{B.10})$$

When  $p_{k,t} = p_k^{\max}$ , i.e.,  $p_{k,t} > p_k^{\min}$ . From (B.7), we have  $\lambda_1 = 0$ . From (B.6), we have

$$\lambda_2 = - \left[ \Delta t \cdot \pi_t + \alpha_t \cdot \frac{(A \cdot p_k^{\max} \cdot \Delta t) \cdot (A \cdot \Delta t)}{\sqrt{(\bar{r}_{k,t} \cdot \Delta t)^2 - (A \cdot p_k^{\max} \cdot \Delta t)^2}} \right] < 0 \quad (\text{B.11})$$



This violates the equation (B.9). When  $p_k^{\min} < p_{k,t} < p_k^{\max}$ , from (B.7) and (B.8), we have  $\lambda_1 = \lambda_2 = 0$ . Equation (B.6) becomes

$$\frac{\partial L}{\partial p_{k,t}} = \Delta t \cdot \pi_t + \alpha_t \cdot \frac{(A \cdot p_{k,t} \cdot \Delta t) \cdot (A \cdot \Delta t)}{\sqrt{(\bar{r}_{k,t} \cdot \Delta t)^2 - (A \cdot p_{k,t} \cdot \Delta t)^2}} = 0, \quad (\text{B.12})$$

which conflicts with

$$\Delta t \cdot \pi_t + \alpha_t \cdot \frac{(A \cdot p_{k,t} \cdot \Delta t) \cdot (A \cdot \Delta t)}{\sqrt{(\bar{r}_{k,t} \cdot \Delta t)^2 - (A \cdot p_{k,t} \cdot \Delta t)^2}} > 0. \quad (\text{B.13})$$

Therefore, the Lagrangian approach and KKT conditions are liable to yield conflicting solutions due to the non-convex function of the monetary compensation. This is the same case when solving the optimization problem of the policy maker with the function of the monetary compensation. To overcome this challenge, our research develops an intelligent heuristic algorithm based on the basic structure of the artificial immune system to search the entire feasible spaces of decision variables for finding the global optimal solutions.

## Appendix B.2. Solution algorithm

Given that the followers of individual generators/consumers optimize their own objective functions separately and simultaneously, a followers-distributed-immune-algorithm (FDIA) is developed. For the multi-objective optimization problem (MOP) of the leader, a leader-multi-objective-immune-algorithm (LMIA) is developed to find the trade-off between leader's objectives. The definitions with respect to the artificial immune system and Pareto optimality are introduced as follows

- **Definition 1 (Antigen-Antibody):** A random vector  $\mathbf{p}$  in the decision variable space  $[\underline{\mathbf{p}}, \bar{\mathbf{p}}]$  is termed as an antigen. The corresponding objective function  $\mathbf{f}(\mathbf{p})$  is termed as an antibody. All vectors generated from the decision variable space form an antigen population as

$$\mathcal{A} = \{\mathbf{p}_1, \dots, \mathbf{p}_{|\mathcal{A}|}\}, \quad (\text{B.14})$$

where  $\mathcal{A}$  is the set of the antigen population, and  $|\mathcal{A}|$  is the number of antigens in this population.

- **Definition 2 (Clone and Mutation):** The clonal process enables more antigens to be reproduced over the decision variable space  $[\underline{\mathbf{p}}, \bar{\mathbf{p}}]$ . Through preserving the diversity of antigens, the entire feasible space of decision variables can be searched to ensure the global optimal solution. The amount of reproduced antigens can be described by the clonal rate as

$$r_c := \left\lfloor \frac{|\mathcal{A}^{\max}|}{|\mathcal{A}|} \right\rfloor, \quad (\text{B.15})$$

where  $r_c$  is the clonal rate,  $|\mathcal{A}^{\max}|$  is the maximum number of antigens in the population, and  $\lfloor \cdot \rfloor$  is the floor function. Hence, each original antigen in (B.14) is cloned by  $(r_c - 1)$  antigens through the mutation process to form the set of the clonal antigen population as

$$\mathcal{A}_c = \{\mathbf{p}_1^1, \dots, \mathbf{p}_1^{r_c-1}, \dots, \mathbf{p}_{|\mathcal{A}|}^1, \dots, \mathbf{p}_{|\mathcal{A}|}^{r_c-1}\}, \quad (\text{B.16})$$

where  $\mathcal{A}_c$  is the set of the clonal antigen population, in which each mutant can be calculated as:  $\vartheta \cdot \mathbf{p} + (1 - \vartheta) \cdot \mathbf{p}'$ , where  $\vartheta \in [0, 1]$  is a random number, and  $\mathbf{p}'$  is a random vector in the decision variable space  $[\underline{\mathbf{p}}, \bar{\mathbf{p}}]$ . Through the clone and mutation process, the antigen population becomes  $\mathcal{A}^{\max} = \mathcal{A} \cup \mathcal{A}_c$ .

- **Definition 3 (Pareto Dominance):** A vector of the objective function  $\mathbf{f}(\mathbf{p}_a)$  dominates another vector of the objective function  $\mathbf{f}(\mathbf{p}_b)$  in the decision variable space  $\mathbf{p}_a, \mathbf{p}_b \in [\underline{\mathbf{p}}, \bar{\mathbf{p}}]$ , denoted as  $\mathbf{f}(\mathbf{p}_a) \leq \mathbf{f}(\mathbf{p}_b)$ , if  $f(p_a) \leq f(p_b)$ ,  $\forall f(p_a) \in \mathbf{f}(\mathbf{p}_a)$ ,  $f(p_b) \in \mathbf{f}(\mathbf{p}_b)$  holds true and at least one inequality is strict. The vector  $\mathbf{f}(\mathbf{p}_b)$  is termed as dominated antibody.

- **Definition 4 (Pareto Optimal Solution):** A vector of decision variable  $\mathbf{p}^* \in [\underline{\mathbf{p}}, \bar{\mathbf{p}}]$  is a Pareto optimal solution, if its objective function  $\mathbf{f}(\mathbf{p}^*)$  dominates all objective functions of any other feasible decision variables in  $[\underline{\mathbf{p}}, \bar{\mathbf{p}}]$ .

- **Definition 5 (Pareto Optimal Set and Pareto Frontier):** The set of all Pareto optimal solutions is termed as the Pareto optimal set, denoted as  $\mathcal{P} = \{\mathbf{p}^*\}$ . The graphical presentation of the objective functions of the Pareto optimal solutions in the Pareto optimal set is termed as the Pareto frontier.

The proposed algorithm is performed over the entire scheduling horizon  $|\mathcal{T}|$  for the following day. During the operation of the artificial immune algorithm, the antigens are randomly generated and cloned to explore the entire decision variable space. In each iteration, the dominated antigen-antibody pairs are removed to keep the non-dominated ones. Until the iteration ends, the antigens of all non-dominated antibodies form the optimal solution. The optimal solution can be yield in polynomial time. The results of each generator/consumer serve as the best solution that maximizes/minimizes its profits/electricity bills, whereas the results of the policy maker serve as a set of Pareto optimal solutions in the Pareto frontier that achieves a trade-off between the carbon revenue neutrality and carbon emissions reduction. Let  $\iota_{\text{FDIA}}$  and  $\iota_{\text{LMIA}}$  denote the nominal numbers of iterations of the FDIA and LMIA, respectively, and  $\iota_{\text{FDIA}}^{\max}$  and  $\iota_{\text{LMIA}}^{\max}$  denote the corresponding maximum numbers of iterations. The pseudocode code of the proposed FDIA-LMIA is shown in **Algorithm 2**.

For comparing the results of the policy maker's MOP, a criterion in [47] is used to select a representative solution from the Pareto frontier. An optimal solution that maximizes the minimum improvement (after normalization) of all objective functions is selected as the representative solution as

$$\mathbf{f}_{\text{rep}} = \max_{\mathbf{p} \in \mathcal{A}} \min_{f \in \mathbf{f}} \frac{\bar{f} - f(\mathbf{p})}{\bar{f} - \underline{f}}, \quad (\text{B.17})$$

where  $\mathbf{f}_{\text{rep}}$  is the vector of representative objective functions form the Pareto frontier,  $\bar{f}$  and  $\underline{f}$  are the minimal and maximal values of each objective function.

## References

- [1] S. J. Davis, N. S. Lewis, M. Shaner, S. Aggarwal, D. Arent, I. L. Azevedo, S. M. Benson, T. Bradley, J. Brouwer, Y.-M. Chiang, et al., Net-zero emissions energy systems, *Science* 360 (6396) (2018).
- [2] B. Lin, Z. Jia, Impacts of carbon price level in carbon emission trading market, *Appl Energy* 239 (2019) 157–170.



---

**Algorithm 2** FDIA-LMIA
 

---

**input:** minimum monetary compensation rate  $\alpha^{\min}$  and minimum carbon prices  $\pi_{\text{carbon}}^{\min}$

1: initialize the leader's strategies:  $\alpha_t = \alpha^{\min}, \pi_{\text{carbon},t} = \pi_{\text{carbon}}^{\min}$   
 2: **while**  $\Delta r_{k,t}^* \neq 0, \pi_{\text{carbon},t}(t+1) \neq \pi_{\text{carbon},t}(t)$  and  $\alpha_t(t+1) \neq \alpha_t(t)$  **do**

3:   **FDIA:**  
 4:    **Input:** monetary compensation rate  $\alpha_t$ , carbon price  $\pi_{\text{carbon},t}$ , and nominal and maximum number of antigens of followers  $|\mathcal{A}_{\text{follower}}|$  and  $|\mathcal{A}_{\text{follower}}^{\max}|$ , respectively  
 5:    randomly initialize the antigen population of followers within the decision variable space  $[\underline{\mathbf{p}}_{\text{follower}}, \bar{\mathbf{p}}_{\text{follower}}]$  as  $\mathcal{A}_{\text{follower}}(0) = \{\mathbf{p}_{\text{follower},1}, \dots, \mathbf{p}_{\text{follower},|\mathcal{A}_{\text{follower}}|}\}$   
 6:    **while**  $\iota_{\text{FDIA}} \leq \iota_{\text{FDIA}}^{\max}$  **do**  
 7:      implement the clone and mutation operation according to equation (B.16), and the number of current antigens  $|\mathcal{A}_{\text{follower}}(\iota_{\text{FDIA}})|$  increases to  $|\mathcal{A}_{\text{follower}}^{\max}|$   
 8:      remove dominated antibodies and corresponding antigens from  $\mathcal{A}_{\text{follower}}(\iota_{\text{FDIA}})$   
 9:      **while**  $|\mathcal{A}_{\text{follower}}(\iota_{\text{FDIA}})| > |\mathcal{A}_{\text{follower}}|$  **do**  
 10:       remove the antigen-antibody pairs with small avidities according to [48], i.e. remove the vectors of the objective function in a crowded region  
 11:      **end while**  
 12:       $\mathcal{A}_{\text{follower}}(\iota_{\text{FDIA}} + 1) = \mathcal{A}_{\text{follower}}(\iota_{\text{FDIA}}), \iota_{\text{FDIA}} = \iota_{\text{FDIA}} + 1$   
 13:    **end while**  
 14:    **Output:** optimal solution  $\mathbf{p}_{\text{follower}}^*$

15:   **LMIA:**  
 16:    **Input:**  $\mathbf{p}_{\text{follower}}^*, |\mathcal{A}_{\text{leader}}|$ , and  $|\mathcal{A}_{\text{leader}}^{\max}|$   
 17:    randomly initialize the antigen population of the leader within the decision variable space  $[\underline{\mathbf{p}}_{\text{leader}}, \bar{\mathbf{p}}_{\text{leader}}]$  as  $\mathcal{A}_{\text{leader}}(0) = \{\mathbf{p}_{\text{leader},1}, \dots, \mathbf{p}_{\text{leader},|\mathcal{A}_{\text{leader}}|}\}$   
 18:    **while**  $\iota_{\text{LMIA}} \leq \iota_{\text{LMIA}}^{\max}$  **do**  
 19:      implement the clone and mutation operation according to equation (B.16), and the number of current antigens  $|\mathcal{A}_{\text{leader}}(\iota_{\text{LMIA}})|$  increases to  $|\mathcal{A}_{\text{leader}}^{\max}|$   
 20:      remove dominated antibodies and corresponding antigens from  $\mathcal{A}_{\text{leader}}(\iota_{\text{LMIA}})$   
 21:      **while**  $|\mathcal{A}_{\text{leader}}(\iota_{\text{LMIA}})| > |\mathcal{A}_{\text{leader}}|$  **do**  
 22:       remove the antigen-antibody pairs with small avidities according to [48]  
 23:      **end while**  
 24:       $\mathcal{A}_{\text{leader}}(\iota_{\text{LMIA}} + 1) = \mathcal{A}_{\text{leader}}(\iota_{\text{LMIA}}), \iota_{\text{LMIA}} = \iota_{\text{LMIA}} + 1$   
 25:    **end while**  
 26:    **Output:** representative solutions from the Pareto optimal set  $\mathbf{p}_{\text{leader}}^*$

27:    $\iota = \iota + 1, \alpha_t = \alpha_t(\iota + 1), \pi_{\text{carbon},t} = \pi_{\text{carbon},t}(\iota + 1)$

28: **end while**

**output:**  $\pi_{\text{carbon},t}^*, \alpha_t^*, \mathbf{p}_{k,t}^*, r_{k,t}^*, \mathbf{p}_{i,t}^*$ , and  $r_{i,t}^*$ .

---

- [3] Electricity market reform: Contracts for difference, Tech. rep., BEIS (Feb. 2017).
- [4] G. Brusco, A. Burgio, D. Menniti, A. Pinnarelli, N. Sorrentino, The economic viability of a feed-in tariff scheme that solely rewards self-consumption to promote the use of integrated photovoltaic battery systems, *Appl Energy* 183 (2016) 1075–1085.
- [5] G. E. Metcalf, D. Weisbach, The design of a carbon tax, *Harv. Envtl. L. Rev.* 33 (2009) 499.
- [6] A. D. Ellerman, F. J. Convery, C. De Perthuis, Pricing carbon: the European Union emissions trading scheme, Cambridge University Press, 2010.
- [7] State and trends of carbon pricing 2021, Tech. rep., World Bank, Washington, DC: World Bank. (May 2021).
- [8] D. Hirst, Carbon price floor (CPF) and the price support mechanism, Tech. rep., UK Parliament (Jan. 2018).
- [9] Y. Wang, J. Qiu, Y. Tao, X. Zhang, G. Wang, Low-carbon oriented optimal energy dispatch in coupled natural gas and electricity systems, *Appl Energy* 280 (2020) 115948.
- [10] Q. Tan, Y. Ding, Q. Ye, S. Mei, Y. Zhang, Y. Wei, Optimization and evaluation of a dispatch model for an integrated wind-photovoltaic-thermal power system based on dynamic carbon emissions trading, *Appl Energy* 253 (2019) 113598.
- [11] S. Rausch, G. E. Metcalf, J. M. Reilly, Distributional impacts of carbon pricing: A general equilibrium approach with micro-data for households, *Energy Econ* 33 (2011) S20–S33.
- [12] J. Fan, J. Li, Y. Wu, S. Wang, D. Zhao, The effects of allowance price on energy demand under a personal carbon trading scheme, *Appl Energy* 170 (2016) 242–249.
- [13] Q. Xu, B. F. Hobbs, Economic efficiency of alternative border carbon adjustment schemes: A case study of california carbon pricing and the western north american power market, *Energy Policy* 156 (2021) 112463.
- [14] M. Yu, S. H. Hong, Incentive-based demand response considering hierarchical electricity market: A stackelberg game approach, *Appl Energy* 203 (2017) 267–279.
- [15] Y. Li, C. Wang, G. Li, C. Chen, Optimal scheduling of integrated demand response-enabled integrated energy systems with uncertain renewable generations: A stackelberg game approach, *Energy Convers Manage* 235 (2021) 113996.
- [16] X. Song, Y. Wang, Z. Zhang, C. Shen, F. Peña-Mora, Economic-environmental equilibrium-based bi-level dispatch strategy towards integrated electricity and natural gas systems, *Appl Energy* 281 (2021) 116142.
- [17] L. Thomas, Y. Zhou, C. Long, J. Wu, N. Jenkins, A general form of smart contract for decentralized energy systems management, *Nat Energy* 4 (2) (2019) 140–149.
- [18] K. Christidis, M. Devetsikiotis, Blockchains and smart contracts for the internet of things, *IEEE Access* 4 (2016) 2292–2303.
- [19] V. Buterin, et al., A next-generation smart contract and decentralized application platform, White Paper 3 (37) (2014).
- [20] M. Foti, C. Mavromatis, M. Vavalis, Decentralized blockchain-based consensus for optimal power flow solutions, *Appl Energy* 283 (2021) 116100.
- [21] G. Liang, S. R. Weller, F. Luo, J. Zhao, Z. Y. Dong, Distributed blockchain-based data protection framework for modern power systems against cyber attacks, *IEEE Trans Smart Grid* 10 (3) (2019) 3162–3173.
- [22] Y. Li, W. Yang, P. He, C. Chen, X. Wang, Design and management of a distributed hybrid energy system through smart contract and blockchain, *Appl Energy* 248 (2019) 390–405.
- [23] F. Luo, Z. Y. Dong, G. Liang, J. Murata, Z. Xu, A distributed electricity trading system in active distribution networks based on multi-agent coalition and blockchain, *IEEE Trans Power Syst* 34 (5) (2019) 4097–4108.
- [24] D. Li, W. Chiu, H. Sun, H. V. Poor, Multiobjective optimization for demand side management program in smart grid, *IEEE Trans Ind Inform* 14 (4) (2018) 1482–1490.
- [25] <https://www.gov.uk/government/publications/participating-in-the-uk-ets/participating-in-the-uk-ets> (Sep. 2021).
- [26] Power stations in the United Kingdom, Tech. rep., Department for Business, Energy & Industrial Strategy (Jul. 2021).
- [27] L. P. Kunjumammed, B. C. Pal, N. F. Thornhill, A test system model for stability studies of UK power grid, in: 2013 IEEE Grenoble Conference, 2013, pp. 1–6.
- [28] R. C. Thomson, G. P. Harrison, J. P. Chick, Marginal greenhouse gas

- emissions displacement of wind power in Great Britain, *Energy Policy* 101 (2017) 201–210.
- [29] A. D. Hawkes, Estimating marginal CO<sub>2</sub> emissions rates for national electricity systems, *Energy Policy* 38 (10) (2010) 5977–5987.
  - [30] N. E. Koltsaklis, A. S. Dagoumas, State-of-the-art generation expansion planning: A review, *Appl Energy* 230 (2018) 563–589.
  - [31] Electricity generation costs, Tech. rep., Department for Business, Energy and Industrial Strategy (Nov. 2020).
  - [32] C. Kang, T. Zhou, Q. Chen, J. Wang, Y. Sun, Q. Xia, H. Yan, Carbon emission flow from generation to demand: A network-based model, *IEEE Trans Smart Grid* 6 (5) (2015) 2386–2394.
  - [33] W. Hua, J. Jiang, H. Sun, J. Wu, A blockchain based peer-to-peer trading framework integrating energy and carbon markets, *Appl Energy* 279 (2020) 115539.
  - [34] B. Murray, N. Rivers, British Columbias revenue-neutral carbon tax: A review of the latest grand experiment in environmental policy, *Energy Policy* 86 (2015) 674–683.
  - [35] R. Jing, M. N. Xie, F. X. Wang, L. X. Chen, Fair p2p energy trading between residential and commercial multi-energy systems enabling integrated demand-side management, *Appl Energy* 262 (2020) 114551.
  - [36] M. Breton, A. Alj, A. Haurie, Sequential stackelberg equilibria in two-person games, *J Optimiz Theory and App* 59 (1) (1988) 71–97.
  - [37] H. Wang, C. E. Murillo-Sanchez, R. D. Zimmerman, R. J. Thomas, On computational issues of market-based optimal power flow, *IEEE Trans Power Syst* 22 (3) (2007) 1185–1193.
  - [38] D. S. Kirschen, G. Strbac, P. Cumperayot, D. de Paiva Mendes, Factoring the elasticity of demand in electricity prices, *IEEE Trans Power Syst* 15 (2) (2000) 612–617.
  - [39] G. Wood, Ethereum: A secure decentralised generalised transaction ledger, *Ethereum Project Yellow Paper* 151 (2014) 1–32.
  - [40] M. Jakobsson, A. Juels, Proofs of work and bread pudding protocols, in: *Secure information networks*, Springer, 1999, pp. 258–272.
  - [41] H. Chen, M. Pendleton, L. Njilla, S. Xu, A survey on ethereum systems security: Vulnerabilities, attacks, and defenses, *ACM Comput Surv* 53 (3) (2020) 1–43.
  - [42] A. Kiayias, A. Russell, B. David, R. Oliynykov, Ouroboros: A provably secure proof-of-stake blockchain protocol, in: *Annual International Cryptology Conference*, Springer, 2017, pp. 357–388.
  - [43] <https://www.gov.uk/government/statistics> (Sep. 2021).
  - [44] <https://www.gridwatch.templar.co.uk/download.php> (Sep. 2021).
  - [45] <https://www.ofgem.gov.uk/data-portal> (Sep. 2021).
  - [46] J. Bialek, Tracing the flow of electricity, *IEE P-Gener Transm D* 143 (4) (1996) 313–320.
  - [47] W. Chiu, H. Sun, H. Vincent Poor, A multiobjective approach to multimicrogrid system design, *IEEE Trans Smart Grid* 6 (5) (2015) 2263–2272.
  - [48] R. Shang, L. Jiao, F. Liu, W. Ma, A novel immune clonal algorithm for mo problems, *IEEE Trans Evol Comput* 16 (1) (2012) 35–50.